Formation flying of pico-satellites

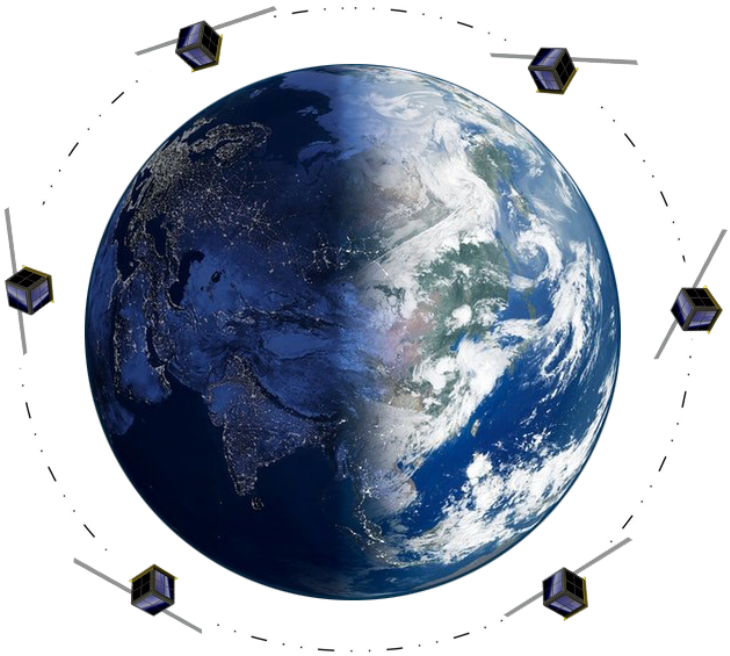

Group 17gr931

Aalborg University
Control & Automation
Fredrik Bajers Vej 7
DK-9220 Aalborg

AALBORG UNIVERSITY
STUDENT REPORT

9th Semester, Project

School of Information and

Communication Technologies

Control and Automation

Fredrik Bajers Vej 7C

9220 Aalborg

en.aau.dk/education/master/control-automation

Title:
Formation flying of pico-satellites

Theme:
Complex systems

Project Period:
P9, Fall 2017
01/09/2017 - 20/12/2017

Project Group:
931

Participants:
- Thibaud Peers
- Nikolaos Biniakos
- Alexandru-Cosmin Nicolae

Supervisors:
Jesper Abilgaard Larsen

Prints: -
Pages: -
Appendices: - (- pages)
Attached: 1 zip file
Concluded: 20/12/2017

Synopsis

This report describes the design and simulation of a control system on a AAU-CubeSat, which is a pico- satellite used for Low Earth Orbit flight.
The objective is to use a flight formation for monitoring Greenland, by having eight satellites equally distributed in orbit.
Two controllers must be designed, one to control the angle between the satellites using the drag force, and one for attitude control. The drag force applied on the satellite depends on the cross section area which can be controlled using the orientation of the satellite.
A linear and a non-linear control method have been designed in order to compare the differences between them.

Preface

This report has been written by group 931 on third semester in Control and Automation on Aalborg University. References made before a full stop regards the sentence and reference after full stop regards the paragraph. Quotes are inside quotations marks and in cursive. Attached to report is a zip file with:

- -
- -
- -
- -

Report by:

Thibaud Peers

Nikolaos Biniakos

Alexandru-Cosmin Nicolae

Contents

1 | Introduction

In the last decades, the space technology is continuously growing. The reason for this is the increased deploying of satellites used in the numerous fields, in particular, telecommunications and meteorology. [1]

Missions containing several satellites are commonly referred to as flying formation, which is known as a distributed satellite system. Two types of distributed space systems are identified as formations and constellations flying.

A distributed space system is defined by NASA Goddard Space Flight Center (GSFC) as *"an end-to-end system including two or more space vehicles and a cooperative infrastructure for scientific measurement, data acquisition, processing, analysis, and distribution"*. [2]

Satellite formation flying is not having a precise definition, however, the definition proposed by NASA GSFC is that *"formation flight involves the use of an active control scheme to maintain the relative positions of the spacecraft "*. In contrast, a constellation is defined as *"two or more spacecraft in similar orbits with no active control by either to maintain a relative position"*. [3]

Formation flying it might offer many possibilities for space exploration, such as surveillance, field measurements and atmospheric survey missions as well as on-orbit satellite inspection, maintenance, and recovery. This approach it has a few challenges which involve autonomous control of the satellites influenced by the different disturbing forces caused by solar radiation pressure, aerodynamic drag, and Earth's oblateness effect, with a purpose of achieving it with minimum fuel consumption. Nevertheless, there is currently no formation flying satellites in orbit, however, two such missions are ESA's "Cluster" mission and the ESA/NASA "Grace" mission, which are in development stages. [3]

The use of satellite formations is expected to rise in the next years. This makes it relevant to look at improving or adding functionalities to satellites. Based on this it has been decided to look at the case of a distributed space system consisting of a formation of eight satellites equally distributed on the orbit and analyzing the behavior between them.

1.1 Problem statement

Design and simulation of a control scheme which maintain a constant angle between satellites by controlling the attitude of each agent.

1.2 Use-case

In this project, the concept of a formation flight of satellites will be used for the purpose of monitoring. Denmark has a small island called Greenland, where the Danish Government needs to monitor it. One method is to have a formation of satellites pointing towards Greenland when they are located above target.

One of the essentials in formation flight is choosing the number of satellites in orbit. Therefore, in order to have a continuous coverage, a distributed satellite system composed of eight satellites equally distributed are chosen, compared with two or four satellites where communication between each other will be poor.

The task the satellite has to perform is acquiring data by flying around Greenland, using radio signals and taking pictures.

2 | System Description

The overall idea of the project is to consider several satellites flying in formation, with an angle in between and with the purpose of maintaining the angle by using the drag force. As a proof of concept, an AAU-CubeSat will be used, by choosing eight AAU-CubeSat that orbits the Earth as shown in *figure 2.1*. In this project, all CubeSat's will be assumed identical. Moreover, a full-scale implementation of the system will not be possible, therefore, the whole system will be simulated using MATLAB and Simulink.

Figure 2.1: Eight satellites in flying formation on orbit

2.1 About AAU-CubeSat

The AAU-CubeSat shown in *figure 2.2* is a pico-satellite developed by Stanford University, assembled at Aalborg University by students and used mainly for Low Earth Orbit (LEO) tests.

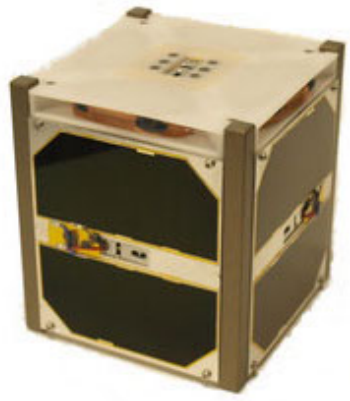

Figure 2.2: View of CubeSat satellite [4]

The pico-satellite is designed for LEO, therefore a few constraints are imposed. The CubeSat is limited in size and weight. The dimensions of the satellite are $10cm \times 10cm \times 10cm$, while the weight is around 1 kg.[5]

In order to place the CubeSat on orbit, a deployment system is used, called P-POD. This system uses the force of a spring to launch the satellite into space. The satellite will be placed inside the launch rocket as payload. By using this system, an important advantage is reducing the cost of the launch. [6]

2.2 AAU-CubeSat actuators

The selection of attitude control components is important in order to meet the performance requirements. For this project, three magnetorquers and three momentum wheels have been chosen as actuators. Initially, using only three momentum wheels has been considered, but the downside of using only momentum wheels is that some amount of momentum can be stored in the wheels, which will imply having a way to take back all that momentum. Therefore, a way get rid of saturation in the wheels is to use external torques (magnetorquers).

Magnetorquers are wire coils which generate an electromagnetic field. The field interacts with the Earth magnetic field and a torque is generated for stabilizing the satellite. An important aspect of the magnetorquer is when a reaction wheel reaches a maximum speed and can no longer produce the torque this is referred as wheel saturation, so a magnetorquer is used to extract the momentum from the wheel.

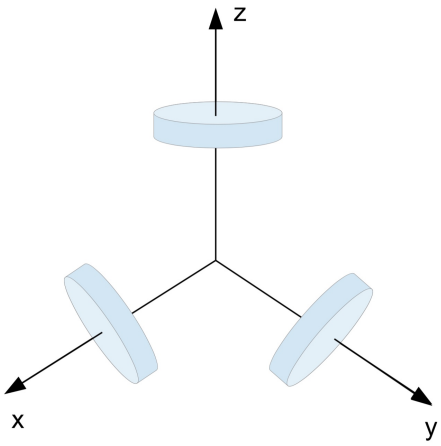

Figure 2.3: Example of three reaction wheel for CubeSat

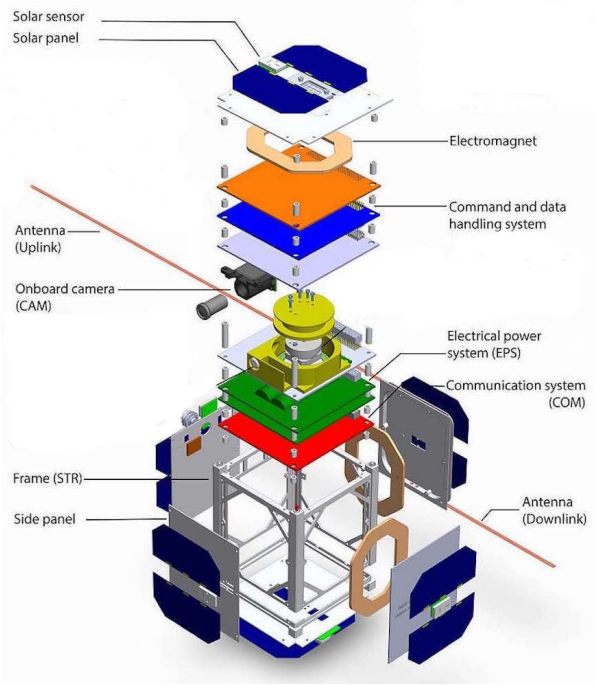

Figure 2.4: Expanded view for CubeSat [7]

Reaction wheels shown in *figure 2.3* strength is that no information is needed about the magnetic field in order to control the CubeSat torque. These wheels are capable to store the momentum needed for manoeuvring or pointing.

2.3 AAU-CubeSat sensors

The CubeSat can sustain itself using solar panels. In the middle of solar panels, a sun sensor similar in figure 2.4 provides a vector equal to the direction of the sun and also a vector of the Earth's magnetic field measured by the magnetometer. Whether the Earth's magnetic field is measured, or the sun vector, the objective is to use these sensors to deliver vector solutions for determining the satellite's orientation and rotation rates.

A **magnetometer** is a sensor used for attitude control, which measures the direction and intensity of the magnetic field. The attitude is determined from the magnetometer by comparing the measured magnetic field with a reference field.

Sun sensor is used for estimating the position of the Sun and delivering a vector of measurements from the Sun.

2.4 Coordinate frames

In order to determine the attitude in three-dimensional space, three different coordinate frames are defined.

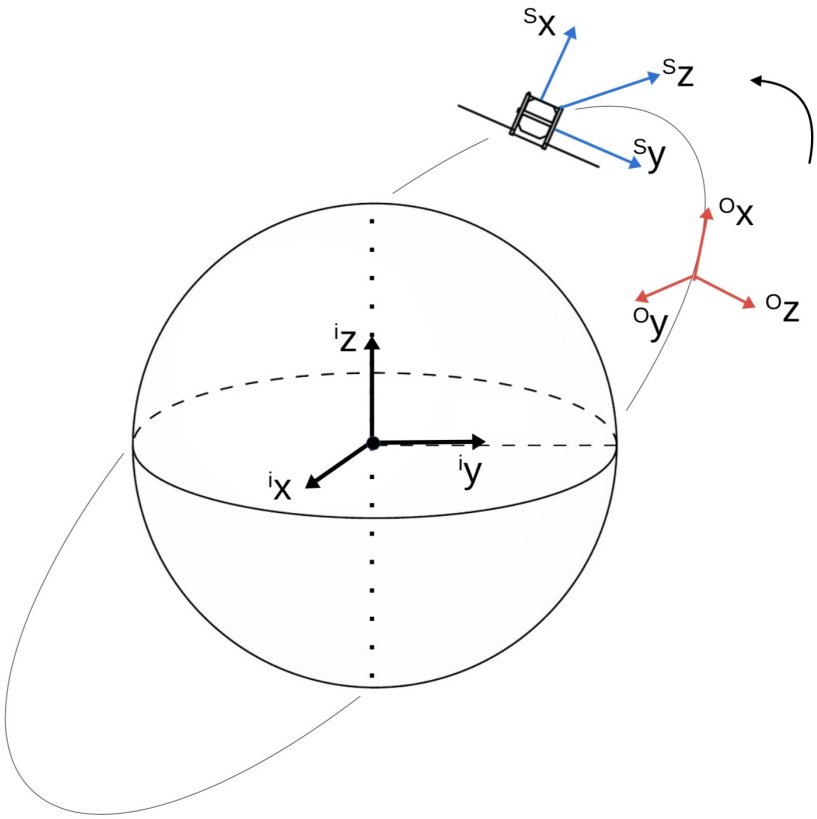

Figure 2.5: Representation of the three coordinate frames

Earth Centered Inertial frame(ECI)

The equations of motion that describe the formation satellite are used in the ECI frame shown in *figure 2.5*, since it can be seen as a non-accelerating frame. The ${}^{i}z$ axis is pointing through the geographical north pole, the ${}^{i}x$ axis is crossing from the point where the equatorial of the earth and the vernal equinox met and the ${}^{i}y$ axis is the cross product of ${}^{i}x$ and ${}^{i}z$ creating a right-handed coordinate system.

Orbit Reference frame(ORF)

The orbit reference shown in *figure 2.5* is placed in the centre of the satellite and defined with the ${}^{o}y$ axis always pointing at the Nadir point, the ${}^{o}x$ axis is tanget to the orbit in the direction of the satellite velocity and ${}^{o}z$ is the cross product of the ${}^{o}x$ and ${}^{o}y$.

Satellite Body Frame(SBF)

The satellite body frame is placed in the centre of mass of the satellite as shown in *figure 2.5* and the axis is defined as represented in *figure 2.6* and rotating with the satellite.

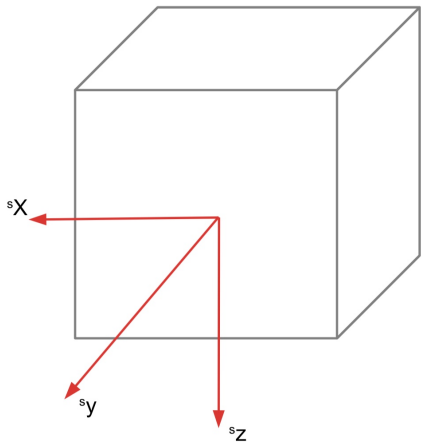

Figure 2.6: Satellite Body Frame

3 | Requirements

Based on the use-case introduced and the available system a set of requirements are formulated.

System requirements

1. **The formation shall be able to maintain a given angle within 45°.**

   The system of satellites shall be able to create a formation around the Earth where the angle between them will be equal.

2. **Each satellite shall be able to change its orientation.**

   The satellites shall be able to rotate using momentum wheels to point towards the desired direction in order to apply the expected drag force.

4 | Angle control between satellites

In this chapter, the focus will be on modelling and the control of the angle between two satellites using the drag force as the control input of the system. The satellite is assumed to be able to change its orientation instantaneously, therefore the drag force can be modified instantaneously. The Earth and the satellite are assumed to be a point mass to simplify the system.

4.1 Modelling

The satellite is mainly subjected to three forces: the gravity, the drag force and the solar radiation. Thus, the second law of Newton gives:

$$\sum \mathbf{F} = m_{sat}\ \mathbf{a} = \mathbf{F_g} + \mathbf{F_D} + \mathbf{F_{rad}} \tag{4.1}$$

with the gravity modeled by:

$$\mathbf{F}_g = -G\frac{m_{earth}m_{sat}}{||\mathbf{p}||^3}\mathbf{p} \tag{4.2}$$

where $\mathbf{p}$ is the vector position of the satellite from the Earth centre to the mass centre of the satellite in the inertial frame and the expression for $\mathbf{F}_D$ and $\mathbf{F}_{rad}$ are explained in the next section.

Modelling of the control input: Aerodynamic Drag Force

The satellite is subjected to an aerodynamic drag force due to the atmosphere. The collisions with the air cause a force in the opposite direction of the velocity of the satellite. The force was modelled by Lord Rayleigh.[8]

$$\mathbf{F_D} = -\frac{1}{2}\rho\ C_D\ A_\perp||\mathbf{v}||\mathbf{v} \tag{4.3}$$

where ρ is the density of the air, C_D is the drag coefficient, $A_\perp$ is the area that is perpendicular in the direction of the velocity of the satellite $\mathbf{v}$.

The drag coefficient C_D and the perpendicular area $A_\perp$ depend on the orientation of the satellite. Therefore, this force can be used as an input for the control of the position and the velocity of the satellite.

The density of the air depends on the altitude of the satellite and the air temperature, but it is considered to be constant in this case for simplifying the model. ρ is chosen to be equal to $1.454 \cdot 10^{-13} Kg/m^3$ based on the empirical model of the Committee on Space Research (COSPAR) International Reference Atmosphere [8].

The drag coefficient is dependent on the orientation and the maximum value of C_D is equal to 1.05 for a non tilted cubed as shown on *figure 4.1* and equal to 0.80 for an angled cubed [9]. The drag coefficient is assumed to be constant and equal to 1 in order to simplify the equation.

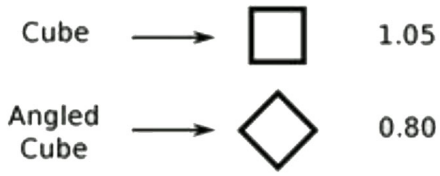

Figure 4.1: Drag coefficient

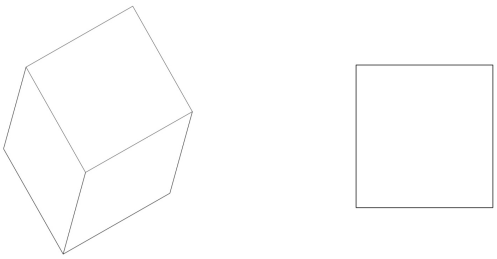

Figure 4.2: Cross sectional area

Therefore, the control parameter is the cross section area $A_\perp$. The maximum and minimum value of $A_\perp$ is represented in *figure 4.2*. Thus, the minimum value is the surface of a square of 10cm of dimension ($A_\perp = 100cm^2$) and the maximum value is equal to $\sqrt{3}\ 100cm^2$. Thus, the drag force can be expressed as the following.

$$\mathbf{F_D} = -u||\mathbf{v}||\mathbf{v} \tag{4.4}$$

where u is the control input and $u \in [7.27 * 10^{-16}, 1.2592 * 10^{-15}]$.

4.2 Disturbance Models

Solar radiation

Solar radiation is emitted constantly by the Sun, which illuminates the surface of the CubeSat. The surface of the satellite will absorb or reflect the solar radiation and will affect the CubeSat and produce a radiation force. [10]

The solar flux can be computed as follows [10]:

$$P = \frac{F_s}{c} \tag{4.5}$$

where F_s is the mean energy flux and it is equal with 1358 W/m^2 and c is the speed of light

The solar radiation $\mathbf{F}_{rad}$ can be expressed as [10]:

$$\mathbf{F_{rad}} = C_a P A \ \frac{\mathbf{r_{sun,sat}}}{||\mathbf{r_{sun,sat}}||} \tag{4.6}$$

where C_a is the surface's reflectance: 0 for a perfect absorber, 2 for a perfect reflector, P is the solar flux, A is the radiated area, $\mathbf{r_{sun,sat}}$ is the vector from the sun to the satellite.

J_2 gravity perturbation

The force which the Earth is exerting upon an object is a conservative force and its potential energy can be written as follows [10]:

$$U(r) = -\frac{\mu}{r} \tag{4.7}$$

Because the Earth is not a perfect sphere and also its mass distribution is not homogeneous, *equation (4.7)* is rewritten as follows [10]:

$$U(r) = -\frac{\mu}{r} + B(r, \phi, \lambda) \tag{4.8}$$

where $B(r, \phi, \lambda)$ is the spherical harmonic expansion used to correct the gravitational potential due to Earth's nonsymmetric mass distribution seen in *figure 4.3*

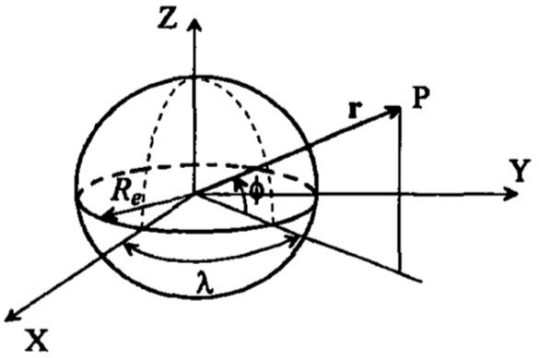

Figure 4.3: Coordinates for deriving the external gravitational potential of the Earth [10]

The expression for gravitational potential of the Earth can be approximate as [10]:

$$U \approx -\frac{\mu}{r}\left[1 - \sum_{n=2}^{\infty}\left(\frac{R_e}{r}\right)^n J_n P_n sin(\phi)\right] = \frac{\mu}{r}[U_0 + U_{J_2} + U_{J_3} + ...] \tag{4.9}$$

where U_0 = -1, $U_{J_2} = \left(\frac{R_e}{r}\right)^2 J_2 \frac{1}{2}(3sin^2\phi - 1)$ and the other terms are neglected

The gravitational forces acting on the satellite are obtained from the relation:

$$\mathbf{F} = -m\nabla U \tag{4.10}$$

and is obtaining the following [1]:

$$F_x = -\frac{\partial U}{\partial x} = \mu\left[-\frac{x}{r^3} + A_{J_2}\left(15\frac{xz^2}{r^7} - 3\frac{x}{r^5}\right)\right] \tag{4.11}$$

$$F_y = -\frac{\partial U}{\partial y} = \mu\left[-\frac{y}{r^3} + A_{J_2}\left(15\frac{yz^2}{r^7} - 3\frac{y}{r^5}\right)\right] \tag{4.12}$$

$$F_z = -\frac{\partial U}{\partial z} = \mu\left[-\frac{z}{r^3} + A_{J_2}\left(15\frac{z^3}{r^7} - 3\frac{z}{r^5}\right)\right] \tag{4.13}$$

where $A_{J_2} = \frac{1}{2}J_2R_e^2$ and and R_e is the mean radius o the Earth at the equator

4.3 Relative dynamics

In order to analyse the distance between two satellites, the relative dynamics are analyzed. Furthermore, to simplify the system, satellites will be assumed to stay on the same plane. This assumption has also to be made due to the limitation of the direction of the input control (the drag force).
To compute the equations of motion of one satellite compared to another, a new frame is used. The frame is illustrated in *figure 4.4*, where the origin is the first satellite and the axis $\hat{\mathbf{x}}$ is defined by $\hat{\mathbf{x}} = \frac{\mathbf{R}}{||\mathbf{R}||}$, where $\mathbf{R}$ is the vector from the centre of the Earth to the first satellite. The axis $\hat{\mathbf{y}}$ is perpendicular to $\hat{\mathbf{x}}$ and in the plane of motion of the satellites and $\hat{\mathbf{z}}$ is defined by the right-hand law ($\hat{\mathbf{z}} = \hat{\mathbf{x}} \times \hat{\mathbf{y}}$).

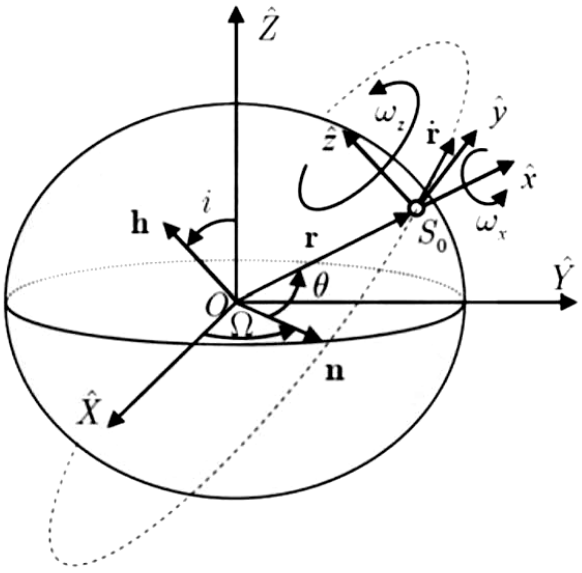

Figure 4.4: Frame for the relative dynamics [2]

Therefore, the vector position from the Earth to the first satellite and the second satellite

can be expressed in this frame:

$$\mathbf{p_1} = R\ \hat{\mathbf{x}} \tag{4.14}$$
$$\mathbf{p_2} = R\ \hat{\mathbf{x}} + x\ \hat{\mathbf{x}} + y\ \hat{\mathbf{y}} \tag{4.15}$$

The relative equation of motion can be writen as follows:

$$\begin{cases} \ddot{x} - 2\dot{y}w - (y+y^*)\dot{w} - (x+x^*)w^2 = \\ \quad -(x+x^*)\dfrac{\mu}{R^3} + \dfrac{u_1}{m}||\dot{\mathbf{p}}_\mathbf{1}||\dot{R} - \dfrac{u_2}{m}||\dot{\mathbf{p}}_\mathbf{2}||(\dot{R} + \dot{x} - (y+y^*)w) + \dfrac{\Delta F_{dist,x}}{m} \\ \ddot{y} + 2\dot{x}w + (x+x^*)\dot{w} - (y+y^*)w^2 = \\ \quad -(y+y^*)\dfrac{\mu}{R^3} + \dfrac{u_1}{m}||\dot{\mathbf{p}}_\mathbf{1}||wR - \dfrac{u_2}{m}||\dot{\mathbf{p}}_\mathbf{2}||(wR + (x+x^*)w + \dot{y}) + \dfrac{\Delta F_{dist,y}}{m} \end{cases} \tag{4.16}$$

The derivation of these equations can be found in *appendix A*.

Relative state space representation

Since the equations of relative motion that have been derived in *appendix A* are not linear, a linearization is made around the operating point, x^* and y^*, by introducing the states with a new variable as $\mathbf{s} = [x\ \dot{x}\ y\ \dot{y}]^\mathsf{T}$. From *equation (4.16)* and assuming that the radius is constant and the angular velocity equals to $w = \sqrt{\frac{\mu}{R^3}}$, a linearization of the system can be derived using some approximations. Moreover, the norm of the velocity of both satellite is assumed to be equal and constant as $||\dot{\mathbf{p}}_\mathbf{1}|| = ||\dot{\mathbf{p}}_\mathbf{2}|| = C$, where $C = \sqrt{\frac{\mu}{R}} = \omega\ R$. Therefore, the nominal system is given by:

$$\begin{cases} \dot{s}_1 = s_2 \\ \dot{s}_2 = 2ws_4 - u_2\dfrac{y^* wC}{m} \\ \dot{s}_3 = s_4 \\ \dot{s}_4 = -2ws_2 - \left(u_2 - u_1\right)\dfrac{wRC}{m} \end{cases} \tag{4.17}$$

using the approximation $\dot{x},\ y \ll y^*$ and $x, x^*,\ \frac{\dot{y}}{w} \ll R$, therefore the system in state space can be writen as:

$$\dot{\mathbf{s}}(t) = \underline{A}\mathbf{s}(t) + \mathbf{B}u(t)$$

$$\underline{A} = \begin{bmatrix} 0 & 1 & 0 & 0 \\ 0 & 0 & 0 & 2w \\ 0 & 0 & 0 & 1 \\ 0 & -2w & 0 & 0 \end{bmatrix}$$

$$\mathbf{B} = \begin{bmatrix} 0 \\ 0 \\ 0 \\ -R^2\ w^2 \end{bmatrix}$$

where $u = u_2 - u_1$. With these assumptions and where u_2 and u_1 are chosen to be equal to u_{max} and u_{min} respectively, therefore, $u > 0$ and in this case, y should decrease as seen in *figure 4.5*. From *figure 4.6*, it can be seen that the approximation and real model of y are not the similar. This is due to the fact that when a satellite is subjected to a drag force, the altitude of the satellite is decreasing and the angular velocity is increasing, which will be proved in the next section.

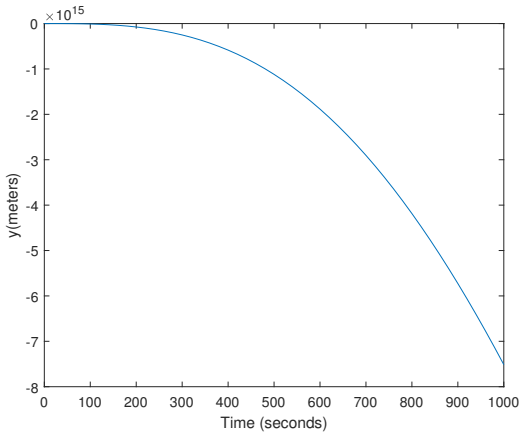

Figure 4.5: Approximation model

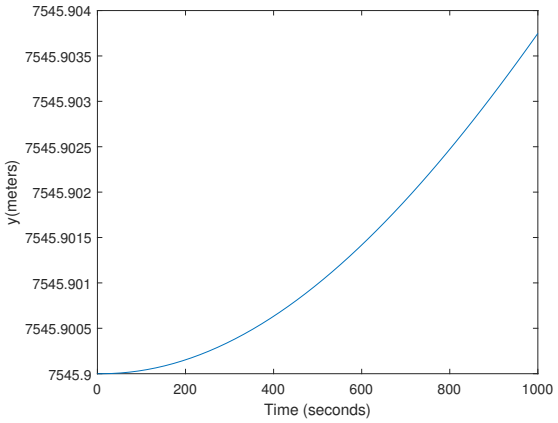

Figure 4.6: Real model

Therefore, when $u_2 > u_1$, then $w_2 > w_1$ this will lead to an increase in the angle θ between the satellites, and since $y = R\ sin\theta$, y will have an increasing attitude. The above mentioned issues are shown in *figure 4.6*.

In conclusion, the approximation that the time derivative of angular velocity is equal to 0 cannot be made for controlling the distance between the two satellites.

4.4 Modelling based on the angular velocity

As seen in the previous section, the angular velocity cannot be assumed constant. Therefore, an equation is needed to estimate it as a function of the drag force. In *appendix B*, the time derivative of the norm of the angular velocity can be approximated as a linear function of the drag force.

$$\Delta\dot{\omega} = Cu \tag{4.18}$$

with $C = \frac{3\omega_0^2 R_0}{m}$. In order to check this equation and the coefficient C, a simulation is performed using a constant drag force coefficient ($u = u_{min}$). The angular velocity as a function of time is shown in *figure 4.7*.

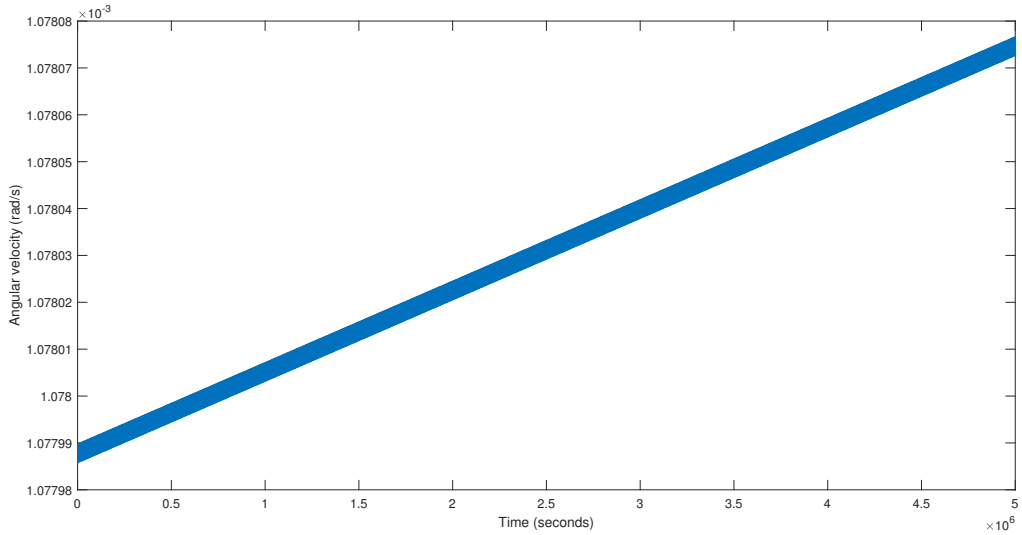

Figure 4.7: Angular velocity as function of time

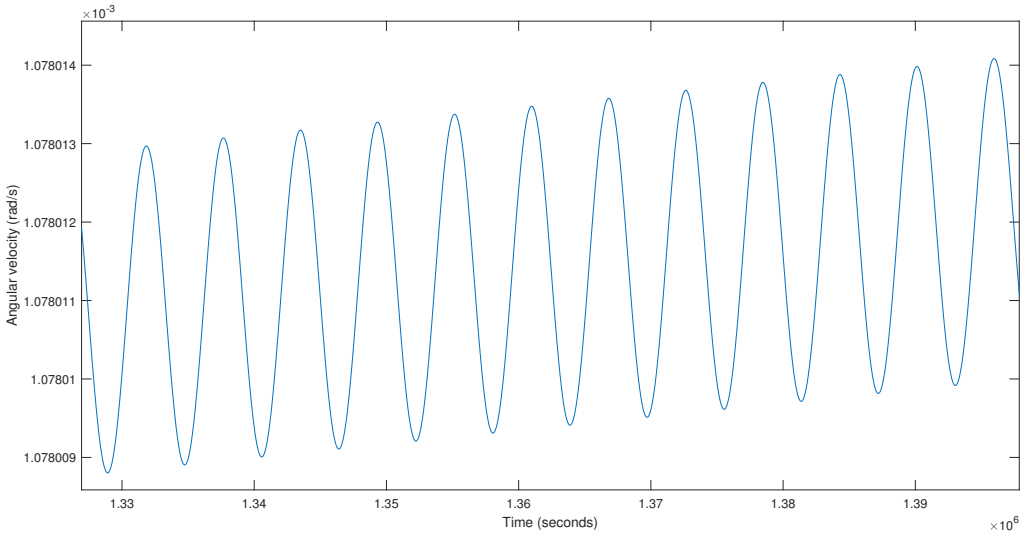

Figure 4.8: Zoom in on the oscillation of the angular velocity

The coefficient found in the simulation is almost the same than in the theory. Oscillations can be observed in *figure 4.8* with a frequency equals to $f \approx \frac{2\pi}{\omega_0}$, where ω_0 is the angular velocity of the satellite in the beginning. This is due to the fact that the orbit is not exactly a circle but an ellipse. Thus, the angular velocity changes slightly during a turn

around the Earth. In order to limit the influence of these variations on the controller, a second order low pass filter is added to reduce the amplitude of these oscillations. A state space representation can be derived with states θ and $\dot{\theta}$, where θ is the angle between two satellites. The time derivative of $\dot{\theta}$ is equal with $\dot{\omega}_2 - \dot{\omega}_1$ and using *equation (4.18)*, $\ddot{\theta} = Cu_2 - Cu_1 = Cu$.

$$\mathbf{s} = \begin{bmatrix} \theta \\ \dot{\theta} \end{bmatrix} \tag{4.19}$$

$$\dot{\mathbf{s}}(t) = \underline{A}s(t) + \mathbf{B}u(t) \tag{4.20}$$

where

$$\underline{A} = \begin{bmatrix} 0 & 1 \\ 0 & 0 \end{bmatrix} \tag{4.21}$$

$$\mathbf{B} = \begin{bmatrix} 0 \\ \frac{3\omega_0^2 R_0}{m} \end{bmatrix} \tag{4.22}$$

4.5 Distance control design

A controller is designed to control the angle between two satellites. Due to the fact that the state representation is linear, Linear Quadratic Regulator(LQR) is chosen as control method with the following cost function:

$$\mathcal{I} = \int (\mathbf{x}^\mathsf{T}\ \underline{Q}\ \mathbf{x} + \mathbf{u}^\mathsf{T}\ \underline{R}\ \mathbf{u})dt \tag{4.23}$$

Due to the fact that no predefined cost is specified, the weighting matrices can be chosen as maximum acceptable values [11], thus, the $\underline{R}$ matrix is defined as $\underline{R} = [u_{delta}^{-2}]$ ($u_{delta} = u_{max} - u_{min}$). For the states weighting matrices, no maximum value is defined. The weight of the second state is chosen to be equal to zero because the desired state to converge is θ and if the first state converges, the second state will also converge to zero. The weight for the first state (θ), is chosen by trial and error leading to the trade off between fast saturation and slow controller since for big values of weights the controller will be in saturation mode faster and with low values, the convergence will be slower. Therefore, the weighting matrices are given by :

$$\underline{Q} = \begin{bmatrix} (\frac{\pi}{7})^{-2} & 0 \\ 0 & 0 \end{bmatrix} \tag{4.24}$$

$$\underline{R} = \left[u_{delta}^{-2}\right] \tag{4.25}$$

The vector of gains K is obtained by solving the Algebraic Riccati equation. The control input signal can be computed ($u = u_2 - u_1$) and therefore if u is bigger than zero, u_1 will be equal to u_{min} and u_2 will be equal to $u + u_{min}$. If u is smaller than zero, it will be the opposite. The control law used for designing the controller is $u = -K(1)\ \theta\ - K(2)\ \dot{\theta}$.

Frequency Analysis

The loop transfer function can be computed $L(s) = P(s)\ C(s)\ LPF(s)\ H_{attittude}(s)$ where $P(s)$ is the transfer function of the state representation system, $C(s) = K_1 + K_2 s$ is the transfer function of the controller, $LPF(s)$ is the transfer function of the second order low pass filter and $H_{attitude}$ is a first order transfer function where the rise time is chosen to be equal to 10 minutes which is an estimation of time that the satellite takes to converge into the good orientation. The bode diagram of L(s) is represented in the *figure 4.9*.

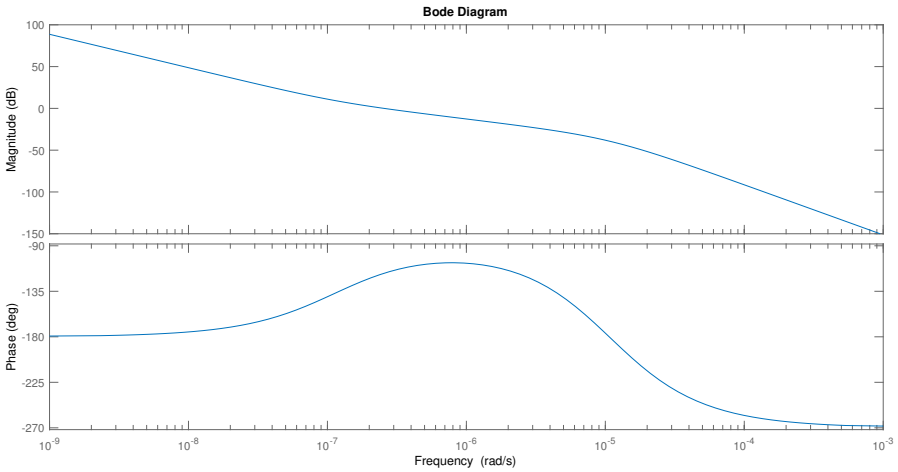

Figure 4.9: Bode diagram of the loop transfer function

The crossover frequency and the phase margin can be extracted from the bode diagram. The crossover frequency is equal to $2.6418 * 10^{-7} \frac{rad}{s}$ and the phase margin is equal to 62.7074° which is enough to accept a large delay due to the small crossover frequency.

Satellite Formation Control

Global algorithm

Since the formation consists of more than two satellites, a second controller is designed to control n satellites around the Earth. The gain vector K computed above can be used to

calculate the difference drag force between two neighbours satellites (called $u_a = u_2 - u_1$, $u_b = u_3 - u_2$, ...). Thus, a system of $n-1$ equations with n unknown variables is obtained. the last equation is chosen to set the minimum value of u_1, u_2,... equals to u_{min}. We have now a system of n equations with n unknown variables that can be solved to determine the drag force coefficient u_i for each satellite. Therefore, to compute the drag force applied on one satellite, the controller needs to know the states of all the other satellites.

Distributed algorithm

In this case, u_1 is chosen to be equal with u_{medium}, therefore u_2 is computed using the control law found in *equation (4.5)*, which is a function of the angle between the first satellite and the second one. The drag force of satellite i can be determined by knowing the angle between the satellite i and $i-1$, the time derivative of this angle and the drag force of the satellite $i-1$.

Stability Analysis

In order to analyze the stability of the distributed formation controller, the global system is written in state space form as in *equation (4.20)*. The states are defined as

$$\mathbf{s} = [\boldsymbol{\theta}_n \ \dot{\boldsymbol{\theta}}_n]^\mathsf{T}$$

where $\boldsymbol{\theta}_n = [\theta_{12} \ \theta_{23} \ \theta_{34} \ \theta_{45} \ \theta_{56} \ \theta_{67} \ \theta_{78}]^\mathsf{T}$ are the angles between neighbour satellites and $\dot{\theta}_n$ is the time derivative of these angles. The system matrix will be a 14x14 matrix and for $i < 8$ satellites, $\dot{s}_i = s_{i+7}$. Therefore the $\underline{A}$ and $\underline{B}$ matrix can be written as:

$$\underline{A} = \left(\begin{array}{c|c} \underline{0}_{(7\times7)} & \underline{I}_{(7\times7)} \\ \hline \underline{0}_{(7\times14)} & \end{array} \right) \tag{4.26}$$

$$\underline{B} = \left(\begin{array}{c} \underline{0}_{(7\times7)} \\ \hline C \ \underline{I}_{(7\times7)} \end{array} \right) \tag{4.27}$$

with the constant $C = \frac{3\omega_0^2 R_0}{m}$ and $\mathbf{u} = [u_2 - u_1; u_3 - u_2; ...; u_8 - u_7]$.

The controller gain that has been found in section 4.5, $\mathbf{K} = [K_1 \ K_2]$, now can be written as $\underline{K}_s = [K_1\underline{I}_{(7\times7)}, \ K_2\underline{I}_{(7\times7)}]$ and by using a control law $u = -\underline{K}\mathbf{s}$ a stability analysis can be made using a Lyapunov candidate function $V = \mathbf{s}^T\mathbf{s}$ where $V > 0$, $\forall \mathbf{s} \neq \mathbf{0}$. Inserting $\underline{K}_s$, the state space equation becomes:

$$\dot{\mathbf{s}} = (\underline{A} + \underline{B}\underline{K}_s)\mathbf{s} \tag{4.28}$$

From Lyapunov stability criterion, it has to be shown that $\dot{V} < 0, \forall s \neq 0$. The derivative of the candidate function can be written as

$$\dot{V} = \dot{\mathbf{s}}^{\mathsf{T}}\mathbf{s} + \mathbf{s}^{\mathsf{T}}\dot{\mathbf{s}} \tag{4.29}$$

and this is equal to:

$$\dot{V} = \mathbf{s}^{\mathsf{T}}(\underline{A} - \underline{BK})^{\mathsf{T}}\mathbf{s} + \mathbf{s}^{\mathsf{T}}(\underline{A} - \underline{BK})\mathbf{s} \tag{4.30}$$

so the only thing that has to be shown in order the system to be stable is to show that the all the eigenvalues of $\underline{A} - \underline{BK} < 0$. The eigenvalues $\underline{A} - \underline{BK}$ were computed and the result was that all eigenvalues have negative real part.
N.B: the drag forces are assumed to not be in saturation.

4.6 Simulation and results

First, the simulation results of the control scheme between two satellites are shown. The reference angle is chosen to be 45^o for the whole formation. The inputs to the controller are $\Delta\theta$ and $\dot{\theta}$, where $\Delta\theta = \theta - \theta_{ref}$ and $\dot{\theta} = w_2 - w_1$. In order to smooth the high frequency oscillations from θ, w_1 and w_2 to the controller a low pass filter is used. The control design is similar to PD controller. In *figure 4.10* is shown the response of the controller and in *figure 4.11* the angle between two satellites. The settling time is 2×10^7 which is equivalent to 230 days which is satisfactory, and also no saturation in the drag force appears.

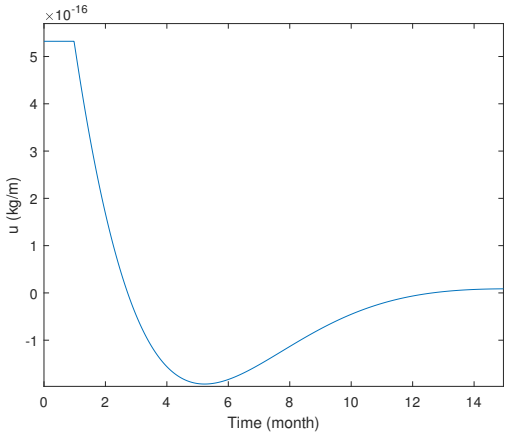

Figure 4.10: Distance control of two satellites

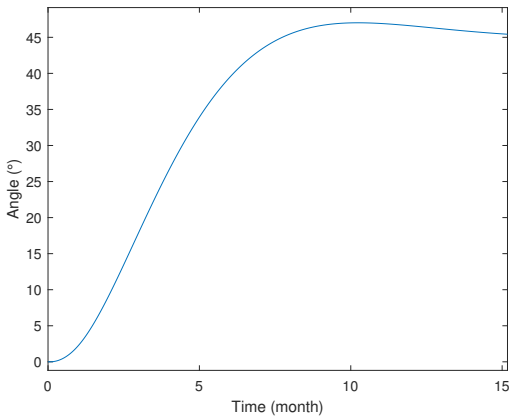

Figure 4.11: Angle between two satellites

The *figure 4.12* and *figure 4.13* show the input signal to the satellite 1 and satellite 2 respectively.

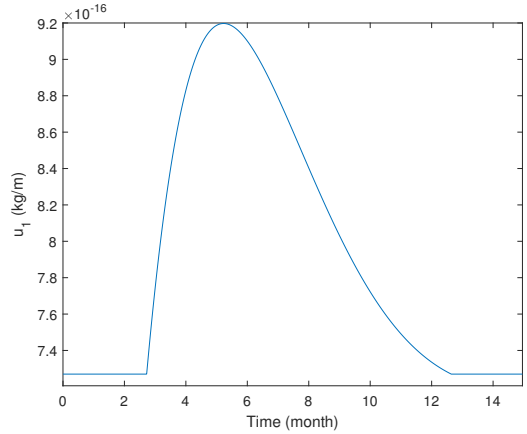

Figure 4.12: The applied input of satellite 1

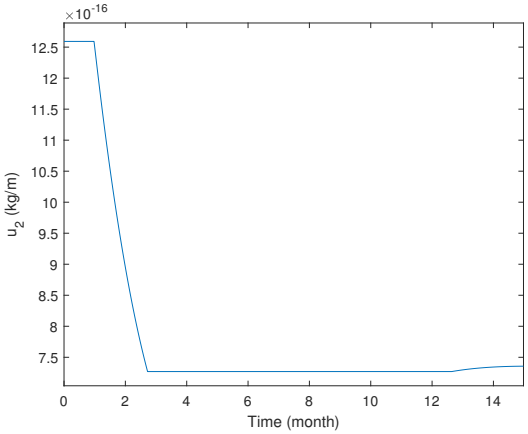

Figure 4.13: The applied input of satellite 2

Global algorithm results

The behaviour of the satellite formation using global algorithm was tested according to a hypothesis that the satellite formation starts at the same place. From *figure 4.14* it can be seen that in the beginning, some saturation appears, but finally, all the satellites converged to the desired angle of 45° .

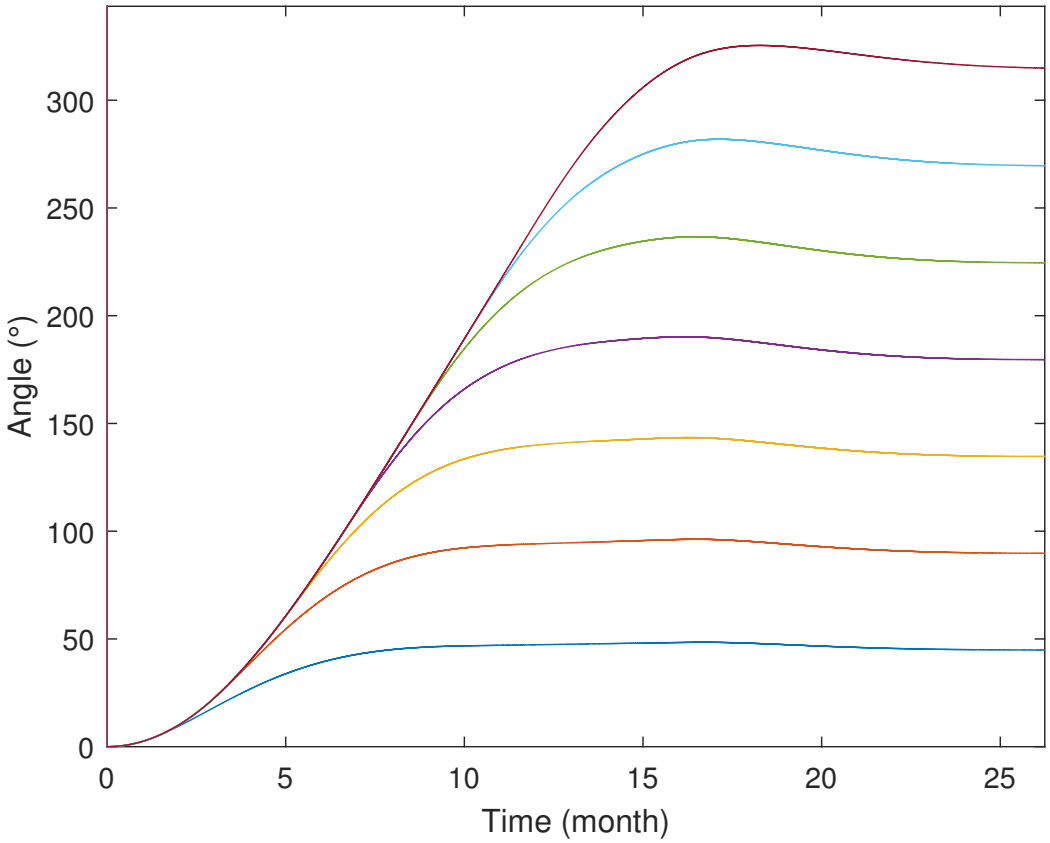

Figure 4.14: Eight satellites in flying formation on orbit

Distributed algorithm results

In the case of a distributed algorithm, the behaviour of the satellite formation is shown in *figure 4.15*, where it can be seen that the overshoot is big, therefore in order to reduce the overshoot, the derivative gain is increased by a factor of 2, which will correct the overshoot as seen in *figure 4.15*.

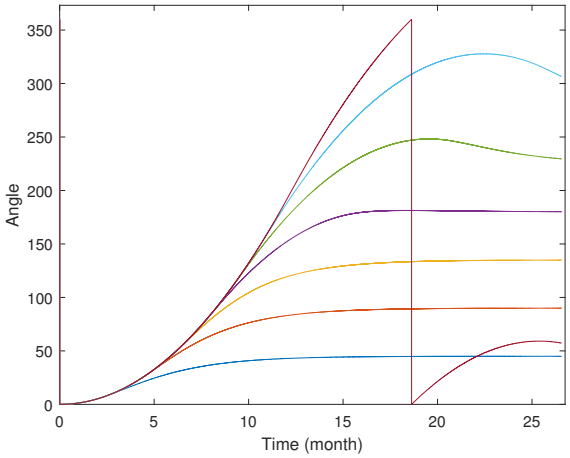

Figure 4.15: Distributed algorithm with overshoot

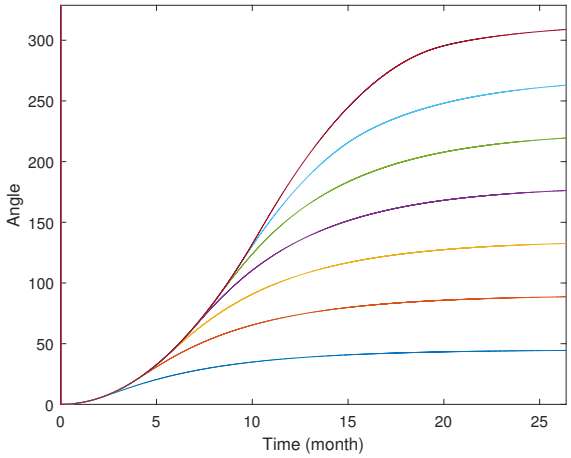

Figure 4.16: Distributed algorithm with corrected gain

The drawback of distributed algorithm is that the angle between satellites will converge slower compared with the global algorithm, moreover, all the satellites are converging to u_{min}, while in the case of distributed algorithm are converging to u_{medium}.

The difference between distributed and global algorithm comes from the fact that the drag force of one satellite is set to constant in the case of distributed algorithm, which leads to less maneuverability, therefore more saturation.

5 | Attitude control

5.1 Modelling

This section provides a description of the dynamic and kinematic equations of motion which constitute the basis for further analysis and description of the forces and disturbances, which may affect a rigid body within LEO. The model for the satellite is derived based on rigid body dynamics and kinematics.

Kinematics

This section will provide the orbit-attitude determination of the satellite using quaternion representation.

Quaternion parameterization is deemed useful for the kinematic analysis of the satellite. The orientation of the rigid body at time t is represented as $\mathbf{q}(t)$ and at time $\mathbf{q}(t + \Delta t)$ is the resulting quaternion at time $t + \Delta t$. The orientation of $\mathbf{q}(t + \Delta t)$ can be found by multiplying the quaternion at time t and the rotations of the satellite during the interval Δt, as follows [10]:

$$ {}^{\mathbf{s}}_{\mathbf{i}}\mathbf{q}(t + \Delta t) = \mathbf{q}(\Delta t) \otimes {}^{\mathbf{s}}_{\mathbf{i}}\mathbf{q}(t) \tag{5.1} $$

where ${}^{\mathbf{s}}_{\mathbf{i}}\mathbf{q}(t + \Delta t)$ is the rotation of the satellite body frame in the inertial frame.

The axis ${}^{\mathbf{s}}\mathbf{x}, {}^{\mathbf{s}}\mathbf{y}, {}^{\mathbf{s}}\mathbf{z}$ are the three axis of the satellite body frame at time t and $[e_x \ e_y \ e_z]$ are the components of the rotation axis unit vector along ${}^{\mathbf{s}}\mathbf{x}, {}^{\mathbf{s}}\mathbf{y}, {}^{\mathbf{s}}\mathbf{z}$. Therefore, $\mathbf{q}(\Delta t)$ can be expresed as [10]:

$$ q_1(\Delta t) = e_x \sin \frac{\Delta \Phi}{2} \tag{5.2} $$

$$ q_2(\Delta t) = e_y \sin \frac{\Delta \Phi}{2} \tag{5.3} $$

$$ q_3(\Delta t) = e_z \sin \frac{\Delta \Phi}{2} \tag{5.4} $$

$$ q_4(\Delta t) = \cos \frac{\Delta \Phi}{2} \tag{5.5} $$

where $\Delta \Phi$ is the rotation at time Δt

Combining the *equation (5.2)* - *equation (5.5)* with *equation (5.1)* results [10]:

$$ {}^{\mathbf{s}}_{\mathbf{i}}\mathbf{q}(t+\Delta t) = \left\{ \cos\frac{\Delta\Phi}{2}\underline{I}_{(4\times4)} + \sin\frac{\Delta\Phi}{2}\begin{bmatrix} 0 & e_z & -e_y & e_x \\ -e_z & 0 & e_x & e_y \\ e_y & -e_x & 0 & e_z \\ -e_x & e_y & -e_z & 0 \end{bmatrix} \right\} {}^{\mathbf{s}}_{\mathbf{i}}\mathbf{q}(t) \tag{5.6} $$

where $\underline{I}$ is the 4×4 identity matrix. Using the small angle approximation for infinitesimal Δt and denoted $\boldsymbol{\omega}$ the instantaneous angular velocity, the sinus and cosinus of $\Delta\phi$ can be approximated as following:

$$ \Delta\phi = \omega\ \Delta t \tag{5.7} $$

$$ \sin\frac{\Delta\Phi}{2} = \frac{\omega\Delta t}{2} \tag{5.8} $$

$$ \cos\frac{\Delta\Phi}{2} = 1 \tag{5.9} $$

$$ \tag{5.10} $$

Therefore, the equation 5.6 becomes:

$$ {}^{\mathbf{s}}_{\mathbf{i}}\mathbf{q}(\mathbf{t}+\boldsymbol{\Delta}\mathbf{t}) = \left[1 + \frac{1}{2}\underline{\Omega}\Delta(t)\right] {}^{\mathbf{s}}_{\mathbf{i}}\mathbf{q}(\mathbf{t}) \tag{5.11} $$

with $\underline{\Omega}$ be the skew symmetric matrix as [10]:

$$ \underline{\Omega} = \begin{bmatrix} 0 & \omega_z & -\omega_y & \omega_x \\ -\omega_z & 0 & \omega_x & \omega_y \\ \omega_y & -\omega_x & 0 & \omega_z \\ -\omega_x & -\omega_y & -\omega_z & 0 \end{bmatrix} \tag{5.12} $$

The time derivative of ${}^{\mathbf{s}}_{\mathbf{i}}\mathbf{q}(\mathbf{t})$ can be computed:

$$ {}^{\mathbf{s}}_{\mathbf{i}}\dot{\mathbf{q}}(\mathbf{t}) = \lim_{\Delta t\to0}\frac{\mathbf{q}(t+\Delta t)-\mathbf{q}(t)}{\Delta t} = \frac{1}{2}\underline{\Omega}\ {}^{\mathbf{s}}_{\mathbf{i}}\mathbf{q}(\mathbf{t}) \tag{5.13} $$

Dynamic Model

In order to describe the behavior of the satellite a dynamic model based on reaction wheels and using Euler's equation of motion has been derived. Euler's equation of motion describing the rotation of a rigid body relates the time derivative of angular momentum to the applied torques and is given by [10]:

$$ \dot{\mathbf{L}} = \mathbf{N_{ext}} = \mathbf{N_{mt}} + \mathbf{N_{dist}} \tag{5.14} $$

where $\mathbf{N_{ext}}$ represents all the external torques caused from the magnetotorque and disturbances, $\boldsymbol{\omega}$ is the angular velocity of the satellite and $\mathbf{L}$ is the total angular momentum of the satellite including reaction wheels, given by:

$$\mathbf{L} = \underline{I}_s\boldsymbol{\omega} + \mathbf{h_{rw}} \tag{5.15}$$

where $\mathbf{h_{rw}}$ is the vector of the angular reaction of the wheels $[h_1\ h_2\ h_3]^T$ in the satellites coordinate system and $\underline{I}_s$ is the inertia matrix of the satellite. The time derivative of $\mathbf{L}$ in the inertial frame can be computed in the satellite body frame as following:

$$\dot{\mathbf{L}} = \dot{\mathbf{L}}_{\mathbf{sat}} + \boldsymbol{\omega} \times \mathbf{L} = \mathbf{N_{mt}} + \mathbf{N_{dist}} \tag{5.16}$$

$$\Leftrightarrow \underline{I}_s\dot{\boldsymbol{\omega}} + \dot{\mathbf{h}}_{\mathbf{rw}} + \boldsymbol{\omega} \times \mathbf{L} = \mathbf{N_{mt}} + \mathbf{N_{dist}} \tag{5.17}$$

$$\Leftrightarrow \dot{\boldsymbol{\omega}} = -\underline{I}_s^{-1}\boldsymbol{\omega} \times \mathbf{L} - \underline{I}_s^{-1}\dot{\mathbf{h}}_{\mathbf{rw}} + \underline{I}_s^{-1}(\mathbf{N_{mt}} + \mathbf{N_{dist}}) \tag{5.18}$$

$$\Leftrightarrow \dot{\boldsymbol{\omega}} = -\underline{I}_s^{-1}\underline{S}(\boldsymbol{\omega})\underline{I}_s\boldsymbol{\omega} - \underline{I}_s^{-1}\underline{S}(\boldsymbol{\omega})\mathbf{h}_{rw} - \underline{I}_s^{-1}\mathbf{N_{rw}} + \underline{I}_s^{-1}(\mathbf{N_{mt}} + \mathbf{N_{dist}}) \tag{5.19}$$

For the ease of notation, the cross product can be written as matrix operation using the $\underline{S}()$ notation representing the skew symmetric matrix given by:

$$\underline{S}(\boldsymbol{\omega}) = \begin{bmatrix} 0 & -\omega_3 & \omega_2 \\ \omega_3 & 0 & -\omega_1 \\ -\omega_2 & \omega_1 & 0 \end{bmatrix} \tag{5.20}$$

The rate of change of angular momentum $\dot{\mathbf{h}}_{\mathbf{mw}}$ is given by Newton's second law for rotation:

$$\dot{\mathbf{h}}_{\mathbf{rv}} = \mathbf{N_{rw}} \tag{5.21}$$

N.B.: In this project, the focus will not be on desinging the magnetotorques and will be set to zero. Therefore, the reaction wheels will be assumed to not have any saturation.

Equation of motion

The behaviour of the satellite attitude is described by the dynamic and kinematic equations, which give a non-linear state space representations.

$$\begin{bmatrix} {}^{\mathbf{s}}_{\mathbf{i}}\dot{\mathbf{q}}(\mathbf{t}) \\ \dot{\boldsymbol{\omega}}(\mathbf{t}) \end{bmatrix} = \begin{bmatrix} \frac{1}{2}\underline{\Omega}_{(4\times4)}\,{}^{\mathbf{s}}_{\mathbf{i}}\mathbf{q}(\mathbf{t}) \\ -\underline{I}_s^{-1}\underline{S}(\boldsymbol{\omega})\underline{I}_s\boldsymbol{\omega}(t) - \underline{I}_s^{-1}\underline{S}(\boldsymbol{\omega})\mathbf{h_{mw}} - \underline{I}_s^{-1}\mathbf{N_{mw}}(t) + \underline{I}_s^{-1}\mathbf{N_{dis}}(t) \end{bmatrix} \tag{5.22}$$

where,
${}^{\mathbf{s}}_{\mathbf{i}}\dot{\mathbf{q}}(\mathbf{t}) = [q_1\ q_2\ q_3\ q_4]^T$
$\dot{\boldsymbol{\omega}}(\mathbf{t}) = [\omega_1\ \omega_2\ \omega_3]^T$
$\underline{\Omega}(\omega)$ is the 4×4 skew symmetric matrix

$\underline{I}_s$ is the inertia matrix
$\underline{S}(\omega)$ is the 3×3 skew symmetric matrix
$\mathbf{N_{dis}}(t)$ is the disturbance torque
$\mathbf{N_{rw}}$ is the torque from reaction wheels

Linearized equation of motion

The kinematic and dynamic equations are linearized around the operating point for the purpose of designing a linear controller. The quaternion $\mathbf{q(t)}$ is split in the operating point ($\bar{\mathbf{q}}$) and the error quaternion ($\tilde{\mathbf{q}}$) and the angular velocity $\boldsymbol{\omega}$ is split in the nominal value $\bar{\boldsymbol{\omega}}$ and the error $\tilde{\boldsymbol{\omega}}$.

$$\begin{aligned}
{}^{\mathbf{s}}_{\mathbf{i}}\mathbf{q} &= {}^{\mathbf{s}}_{\mathbf{i}}\bar{\mathbf{q}} \otimes \tilde{\mathbf{q}} && (5.23)\\
\tilde{\mathbf{q}} &= {}^{\mathbf{s}}_{\mathbf{i}}\bar{\mathbf{q}}^{-1} \otimes {}^{\mathbf{s}}_{\mathbf{i}}\mathbf{q} && (5.24)\\
\boldsymbol{\omega} &= \bar{\boldsymbol{\omega}} + \tilde{\boldsymbol{\omega}} && (5.25)
\end{aligned}$$

Thus, the linearized equation of motion for the satellite are given by [12]:

$$\begin{bmatrix} \dot{{}^{\mathbf{s}}_{\mathbf{i}}\tilde{\mathbf{q}}}(\mathbf{t}) \\ \dot{\tilde{\boldsymbol{\omega}}}(\mathbf{t}) \end{bmatrix} = \begin{bmatrix} -\underline{S}(\bar{\boldsymbol{\omega}}) & \frac{1}{2}\underline{\mathbf{1}}_{(3\times3)} \\ \underline{0}_{(3\times3)} & \underline{I}_s^{-1}\underline{S}(\underline{I}_s\bar{\boldsymbol{\omega}}) - \underline{I}_s^{-1}\underline{S}(\bar{\boldsymbol{\omega}})\underline{I}_s \end{bmatrix} \begin{bmatrix} \tilde{\mathbf{q}}(\mathbf{t}) \\ \tilde{\boldsymbol{\omega}}(t) \end{bmatrix} - \begin{bmatrix} \underline{\mathbf{0}}_{(3\times3)} \\ \underline{I}_s^{-1} \end{bmatrix} \mathbf{N_{rw}} \tag{5.26}$$

5.2 Disturbance Models

Gravity-Gradient torque

An unbalanced satellite in orbit is subjected to a torque due to Earth's non-uniform gravitational field. Assumed that the Earth is a point mass and the satellite is a rigid body, the gravitational torque can be estimated. Each infinitesimal element of the satellite of mass dm_i is subjected to an infinitesimal force $\mathbf{d}F_i$ acting on the mass element located at position $\mathbf{R}i$ from the Earth's geometric centre that can be calculated as [10]:

$$d\mathbf{F_i} = -G\frac{m_{earth}}{\mathbf{R}_i^3}dm_i \cdot \mathbf{R_i} \tag{5.27}$$

where G is the gravitational constant, m_{earth} is the mass of the earth and $\mathbf{R_i}$ is the vector from the Earth's geometric centre to the infinitesimal element of the satellite.

The torque about the geometric centre of the satellite due to a force dF_i at a distance r_i from the geometric centre of the satellite is calculated as [10]:

$$d\mathbf{N_{gra}} = \mathbf{r}_i \times d\mathbf{F_i} \tag{5.28}$$

$\mathbf{r}_i$ can be written as the sum of two vectors as seen in the *figure 5.1*, $\mathbf{r}_{co}$ which is the vector from geometric centre of the satellite to the centre of mass, and $\mathbf{r}_{ci}$ which is the

vector from the centre of mass to the infinitesimal element. Therefore, the expression of the gravity gradient torque is obtained by integrating *equation (5.28)* and thus obtaining [10]:

$$\mathbf{N}_{gra} = \int_{sat} (\mathbf{r}_{co} + \mathbf{r}_{ci}) \times d\mathbf{F_i} \tag{5.29}$$

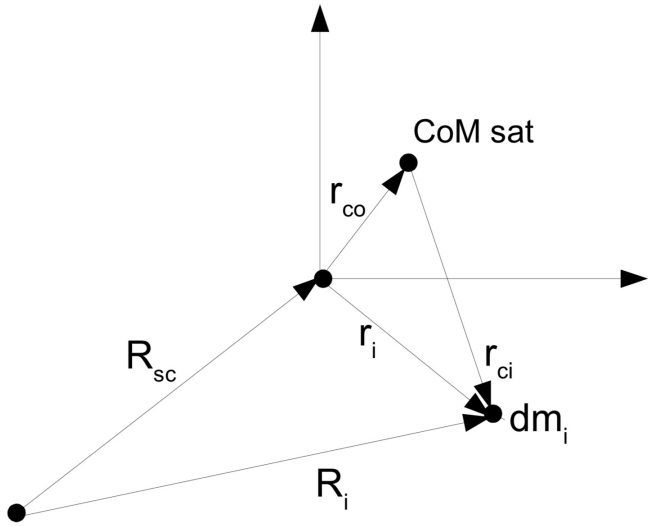

Figure 5.1: Coordinate system for the calculation of gravity gradient torque [10]

The vector $\mathbf{R_i}$ can be written as $\mathbf{R_i} = \mathbf{R_{sc}} + \mathbf{r_i}$. Finally assuming that the geometric centre of the satellite is aligned with its centre of mass, this is equal by setting $r_{co} = 0$, and by using the formula of inertia, and replacing the term dF_i by *equation (5.27)* the gravity gradient torque can be written as [10]:

$$\mathbf{N}_{gra} = \frac{3\mu}{\mathbf{R}_{sc}^3} [\hat{\mathbf{R}}_{\mathbf{sc}} \times (\mathbf{I}\ \hat{\mathbf{R}}_{\mathbf{sc}}] \tag{5.30}$$

where $\hat{\mathbf{R}}_{\mathbf{sc}}$ is the unit vector from the earth's geometric centre to the satellite's geometric centre, and $\underline{I}$ is the diagonal inertia matrix of the satellite.

Solar radiation

The surface of the CubeSat will absorb or reflect the solar radiation, nevertheless, these two situations will alter the CubeSat, which will produce a torque about the satellite centre of mass (CoM). The torque around CoM is given by [10]:

$$\mathbf{N}_{rad} = \mathbf{R}_{CoM} \times \mathbf{F_{rad}} \tag{5.31}$$

where $\mathbf{F}_{rad}$ is the solar radiation and $\mathbf{R}_{CoM}$ is the vector from the centre of mass to the geometric centre of radiation

The solar radiation $\mathbf{F}_{rad}$ can be expressed as [10]:

$$\mathbf{F}_{rad} = C_a P A \, \hat{\mathbf{R}}_{\mathbf{sun,sat}} \tag{5.32}$$

where $\hat{\mathbf{R}}_{\mathbf{sun,sat}}$ is the unit vector with the direction from the sun to the satellite, C_a is the surface's reflectance: 0 for a perfect absorber, 1 for a perfect reflector, while P is the solar flux and A is the radiated area.

Atmospheric drag

For objects in LEO, friction with molecules can have a significant impact on the satellite surface by creating a force which acts upon the satellite surface. [13]

The equation of the atmospheric drag force is already computed as shown in *equation (4.3)*. Since the force has been computed also the torque can be computed by using the cross product between the drag force and the vector from the centre of mass to the centre of pressure of the satellite.

The aerodynamic torque acting on the satellite can be written as [10]:

$$\mathbf{N}_{drag} = \mathbf{r}_s \times \mathbf{F}_D \tag{5.33}$$

where:
$\mathbf{r}_s$ is the vector from the centre of mass to the centre of pressure, where the centre of pressure is equal with the geometric centre of the exposed area
$\mathbf{F}_D$ is the atmospheric drag force

5.3 Attitude control design

Relationship between drag force and quaternion

In order to apply the desired drag force, a function has to be found to compute the associated quaternion. A method to find a bijective function between drag force and quaternion is to find two quaternions that give the minimum and the maximum drag force and analyse the drag force in the path between them.

A quaternion can be defined as a sequence of three rotations around the three axis:

$$\mathbf{q} = \mathbf{q}_x \otimes \mathbf{q}_y \otimes \mathbf{q}_z \tag{5.34}$$

with

$$\mathbf{q}_x = sin\left(\frac{\theta_x}{2}\right) * i + cos\left(\frac{\theta_x}{2}\right) \tag{5.35}$$

$$\mathbf{q}_y = sin\left(\frac{\theta_y}{2}\right) * j + cos\left(\frac{\theta_y}{2}\right) \tag{5.36}$$

$$\mathbf{q}_z = sin\left(\frac{\theta_z}{2}\right) * k + cos\left(\frac{\theta_z}{2}\right) \tag{5.37}$$

The drag force can be computed as the folowing:

$$u = \frac{u_{min}}{A_{min}} A_{\perp}({}^{\mathbf{s}}_{\mathbf{o}}\mathbf{q}) \tag{5.38}$$

$$u = u_{min}\ f({}^{\mathbf{s}}_{\mathbf{o}}\mathbf{q}) \tag{5.39}$$

where $A_{\perp}({}^{\mathbf{s}}_{\mathbf{o}}\mathbf{q})$ is the perpendicular area of the satellite with a rotation ${}^{\mathbf{s}}_{\mathbf{o}}\mathbf{q}$ and $f({}^{\mathbf{s}}_{\mathbf{o}}\mathbf{q})$ is defined by $f = \frac{A_{\perp}}{A_{min}}$. Due to the fact that the velocity of the satellite is along the x axis in the orbit frame, a rotation around this axis doesn't change $A_{\perp}$. Therefore, f can be analysed using only rotation around y and z axes. The graph of f in function of θ_z and θ_y can be seen in *figure 5.2*.

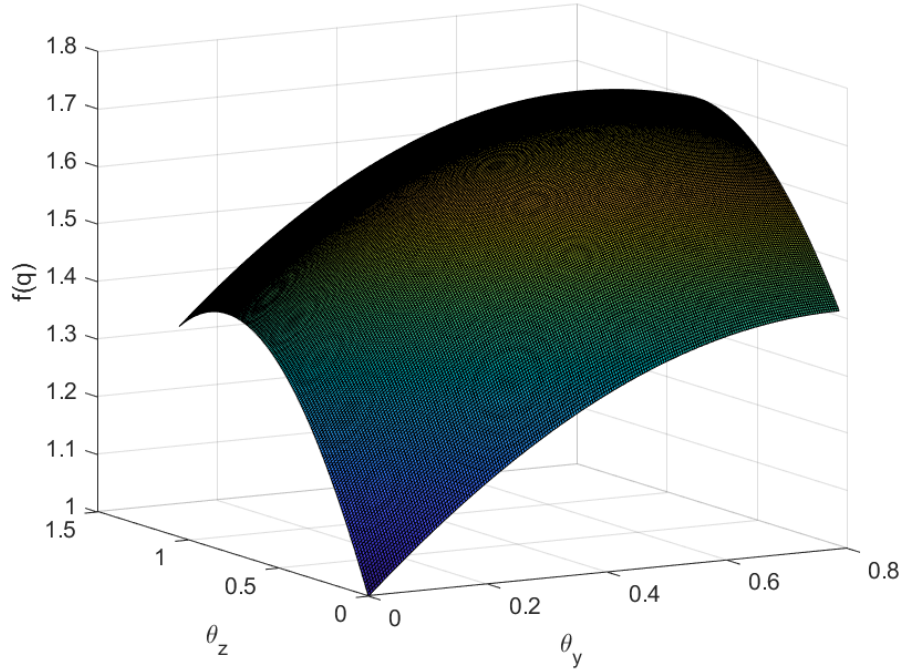

Figure 5.2: Perpendicular area in function of rotations around y and z axes

The quaternion for the minimum drag force is defined by the rotations $\theta_{y,min} = \theta_{z,min} = 0$ and the quaternion that give the maximum drag force is defined by the rotations $\theta_{y,max} = 0.61568$ rad and $\theta_{z,max} = \frac{\pi}{4}$.

Due to the fact that there are no singularities in the path between the minimum and maximum drag force, the function $f({}^{\mathbf{s}}_{\mathbf{o}}\mathbf{q})$ can be computed and analyzed in this path:

$$ {}^{\mathbf{s}}_{\mathbf{o}}\mathbf{q} = {}^{\mathbf{s}}_{\mathbf{o}}\mathbf{q_y} \otimes {}^{\mathbf{s}}_{\mathbf{o}}\mathbf{q_z} \tag{5.40} $$

$$ \tag{5.41} $$

with

$$ \theta_y = \alpha \ \theta_{y,max} \tag{5.42} $$

$$ \theta_z = \alpha \ \theta_{z,max} \tag{5.43} $$

and $\alpha \in [0, 1]$.

The *figure 5.3* shows $f({}^{\mathbf{s}}_{\mathbf{o}}\mathbf{q}(\boldsymbol{\alpha}))$:

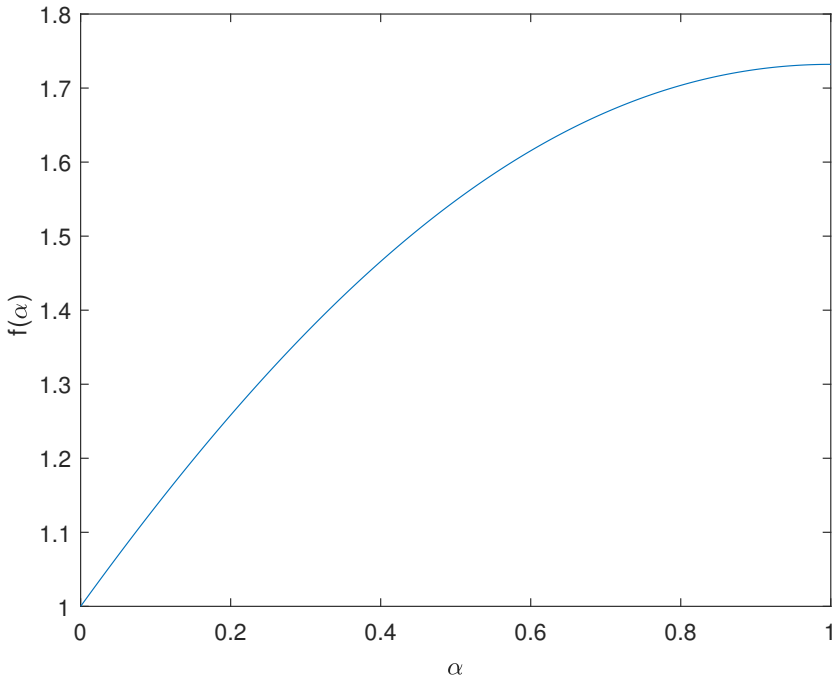

Figure 5.3: Perpendicular area in function of rotations around y and z axes

This function can be approximated by a polynomial of degree two. The relative error of this approximation represented in *figure 5.4* is small and thus, the approximation by a polynomial of degree two can be used.

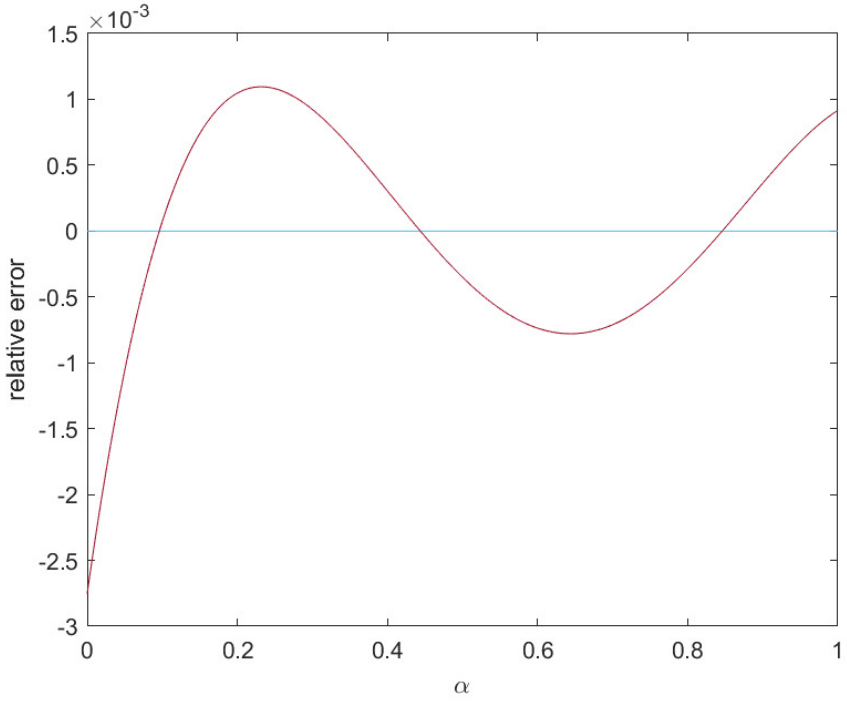

Figure 5.4: Relative error of the fitting approximation

Therefore, the quaternion that give the desired drag force in the orbit frame can be computed by following this algorithm:

$$\frac{u}{u_{min}} = f(\alpha) \approx p_1\alpha^2 + p_2\alpha + p_3 \tag{5.44}$$

$$\Rightarrow \alpha = \frac{-p_2 + \sqrt{p_2^2 - 4p_1\left(p_3 - \frac{u}{u_{min}}\right)}}{2p_1} \tag{5.45}$$

$$\Rightarrow \theta_y = \alpha\theta_{y,max} \tag{5.46}$$

$$\theta_z = \alpha\theta_{z,max} \tag{5.47}$$

$$\Rightarrow {}^{\mathbf{s}}_{\mathbf{o}}\mathbf{q_y} = sin\left(\frac{\theta_y}{2}\right) * j + cos\left(\frac{\theta_y}{2}\right) \tag{5.48}$$

$${}^{\mathbf{s}}_{\mathbf{o}}\mathbf{q_z} = sin\left(\frac{\theta_z}{2}\right) * k + cos\left(\frac{\theta_z}{2}\right) \tag{5.49}$$

$$\Rightarrow {}^{\mathbf{s}}_{\mathbf{o}}\mathbf{q_{ref}} = {}^{\mathbf{s}}_{\mathbf{o}}\mathbf{q_y} \otimes {}^{\mathbf{s}}_{\mathbf{o}}\mathbf{q_z} \tag{5.50}$$

N.B.: This is one solution to the problem, but there is an infinity of quaternions for one drag force. A better solution would be to choose the reference quaternion that gives the desired drag force and that requires the smallest rotation relative to the current position of the satellite. However, this solution is very hard to implement.

Linear Control Design - State Feedback

The linearized *equation (5.26)* of the attitude system allows designing a state feedback control. However, the nominal values of the quaternion and the angular velocity depends on the drag force desired and thus, they aren't constant all over the time. Therefore, the designed control have to stabilize the system for all the possibilities of $\bar{q}$ and $\bar{\omega}$.

The norm of $\bar{\boldsymbol{\omega}}$ is known and is equal to the angular velocity of the satellite around the Earth ($||\bar{\boldsymbol{\omega}}|| \approx 0.0011$). Due to the fact that this value is small compared to $\frac{1}{2}$, the A matrix can be approximated by:

$$\underline{A} \approx \begin{bmatrix} \underline{0}_{(3\times3)} & \frac{1}{2}\underline{1}_{(3\times3)} \\ \underline{0}_{(3\times3)} & \underline{0}_{(3\times3)} \end{bmatrix} \tag{5.51}$$

The system can be split in three subsystems defined by the matrix equation:

$$\begin{bmatrix} \dot{\tilde{q}}_i(t) \\ \dot{\tilde{\omega}}_i(t) \end{bmatrix} = \begin{bmatrix} 0 & \frac{1}{2} \\ 0 & 0 \end{bmatrix} \begin{bmatrix} \tilde{q}_i(t) \\ \tilde{\omega}_i(t) \end{bmatrix} + \begin{bmatrix} 0 \\ I_{i,s}^{-1} \end{bmatrix} N_i \tag{5.52}$$

where $i = 1, 2, 3$.

The input control torque is defined by a state feedback law:

$$N_i = -\begin{bmatrix} k_1 & k_2 \end{bmatrix} \begin{bmatrix} \tilde{q}_i(t) \\ \tilde{\omega}_i(t) \end{bmatrix} \tag{5.53}$$

Therefore,

$$\underline{A} - \underline{BK} = \begin{bmatrix} 0 & \frac{1}{2} \\ -\frac{k_1}{I_{i,s}} & -\frac{k_2}{I_{i,s}} \end{bmatrix} \tag{5.54}$$

Pole Placement

$$det(s\underline{I} - (\underline{A} - \underline{BK})) = s^2 + \frac{k_2}{I_{i,s}}s + \frac{k_1}{2I_{i,s}} \tag{5.55}$$

By identification with a general second order equation $s^2 + 2\zeta\omega_n s + \omega_n^2$ where ζ is the damping factor and ω_n is the natural frequency, the gains are given by:

$$k_1 = -2\ I_{i,s}\ \omega_n^2 \tag{5.56}$$

$$k_2 = -2\ I_{i,s}\ \zeta\ \omega_n \tag{5.57}$$

The damping factor is chosen to be equal to 1 and the rise time is chosen to be equal to 60 and thus $\omega_n = \frac{2\pi}{T_n} = \frac{2\pi}{60/0.35}$. Therefore, all the eigenvalues are equal to -0.0367.

Stability

The stability of control designed in the previous section has to be verified for all $\bar{\boldsymbol{\omega}}$.

$$\underline{A}(\bar{\boldsymbol{\omega}}) = \begin{bmatrix} -\underline{S}(\bar{\boldsymbol{\omega}}) & \frac{1}{2}\mathbf{1}_{(3\times3)} \\ \underline{0}_{(3\times3)} & \underline{I}_s^{-1}\underline{S}(\underline{I}_s\bar{\boldsymbol{\omega}}) - \underline{I}_s^{-1}\underline{S}(\bar{\boldsymbol{\omega}})\underline{I}_s \end{bmatrix} \tag{5.58}$$

Due to the fact that the above A matrix is affine in $\bar{\boldsymbol{\omega}}$, the stability can be only checked on the vertices of the convex polyhedron (cube) that contains all the possibilities of $\bar{\boldsymbol{\omega}}$ as represented in *figure 5.5*. [14]

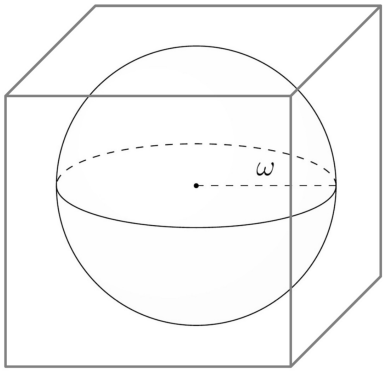

Figure 5.5: Convex Polyhedron

The maximum real part of the eigenvalue in the vertices of the cube is equal -0.0308 that is very close to the desired eigenvalue.

Non linear Control Design - Sliding Mode Control

In parallel to the linear feedback control design, a non-linear method has also been designed. A sliding mode controller is implemented in order to compare the differences

between the two methods. The sliding mode controller brings the system states to a designed manifold s, such that when the states are on the manifold, they will converge to the desired reference. When the states are not on the manifold, a control law that drives the states to the manifold is necessary. The satellite motion can be represented to the space of the sliding variable s. The sliding variable can be written in terms of the signal deviation as derived in *equation (5.25)*.The quaternion error can be written as [15]:

$$\tilde{\mathbf{q}} = \bar{\mathbf{q}}^{-1} \otimes \mathbf{q} = \begin{bmatrix} q_{4r} & q_{3r} & -q_{2r} & q_{1r} \\ -q_{3r} & q_{4r} & q_{1r} & q_{2r} \\ q_{2r} & -q_{1r} & q_{4r} & q_{3r} \\ -q_{1r} & -q_{2r} & -q_{3r} & q_{4r} \end{bmatrix} \begin{bmatrix} q_1 \\ q_2 \\ q_3 \\ q_4 \end{bmatrix} \tag{5.59}$$

where $\bar{\mathbf{q}}$ represents the quaternion reference and $\mathbf{q}$ the measured quaternion. The time derivative of the error quaternion is given by [16]:

$$\dot{\tilde{\mathbf{q}}} = \frac{1}{2}\Big(- \mathbf{q}_{\bar{\omega}} \otimes \tilde{\mathbf{q}} + \tilde{\mathbf{q}} \otimes \mathbf{q}_{\bar{\omega}} + \tilde{\mathbf{q}} \otimes \mathbf{q}_{\tilde{\omega}} \Big) \tag{5.60}$$

where $\mathbf{q}_{\bar{\omega}} = \bar{\omega_1} * i + \bar{\omega_2} * j + \bar{\omega_3} * k + 0$ and $\mathbf{q}_{\tilde{\omega}} = \tilde{\omega_1} * i + \tilde{\omega_2} * j + \tilde{\omega_3} * k + 0$. By choosing the sliding manifold variable to be equal:

$$s = F\tilde{\mathbf{q}} + \tilde{\boldsymbol{\omega}} \tag{5.61}$$

where $F = d * diag[1\ 1\ 1]$ is positive definite. The angular velocity error can be written as $\tilde{\boldsymbol{\omega}} = \boldsymbol{\omega} - \bar{\boldsymbol{\omega}}$. Therefore, when s = $\mathbf{0}$, $\tilde{\boldsymbol{\omega}} = -d * \tilde{\mathbf{q}}_{\mathbf{1:3}}$ and thus the time derivative of the real part of the error quaternion is computed from the equation 5.60:

$$\dot{\tilde{q}}_4 = -\frac{1}{2}\tilde{\boldsymbol{\omega}} \cdot \tilde{\mathbf{q}}_{\mathbf{1:3}} \tag{5.62}$$

$$= \frac{d}{2}||\tilde{\mathbf{q}}_{1:3}||^2 \tag{5.63}$$

$$= \frac{d}{2}\Big(1 - \tilde{q}_4^2\Big) \tag{5.64}$$

According to equation 5.64, $\tilde{\mathbf{q}}$ will converge to $[0; 0; 0; 1]$ and d can be designed by trial and error to have the desired convergence. The behaviour of $\tilde{q}_4$ with d equal to 0.035 is represented in the *figure 5.6*.

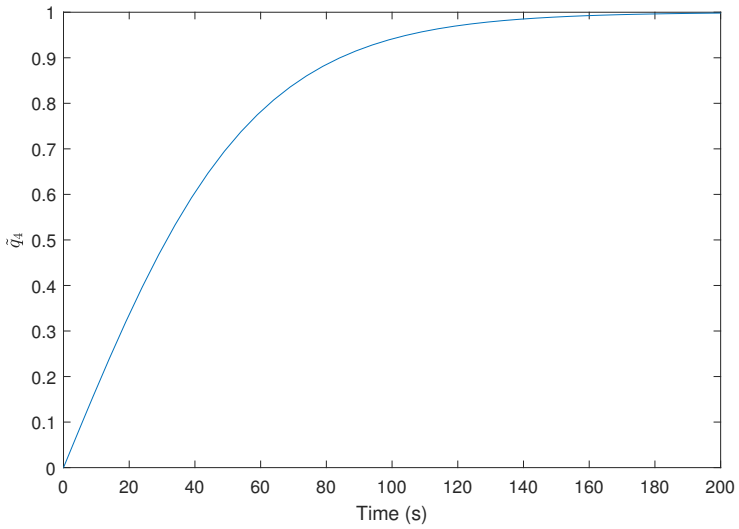

Figure 5.6: $\tilde{q}_4$ in function of time with d = 0.035

Considering the Lyapunov candidate function as:

$$V = \frac{1}{2}\mathbf{s^T s} \tag{5.65}$$

The time derivative of the Lyapunov fuction can be written as:

$$\dot{V} = \frac{1}{2}\left(\dot{\mathbf{s}^\mathbf{T}}\mathbf{s} + \mathbf{s^T}\dot{\mathbf{s}}\right) \tag{5.66}$$

In order to prove stability it has to be shown that $\dot{V} < 0 \ \forall s \neq 0$ this is equal by showing:

$$\mathbf{s^T}\dot{\mathbf{s}} < 0 \ \forall \mathbf{s} \neq 0 \tag{5.67}$$

The *equation (5.61)* is substitute

$$\dot{V} = \mathbf{s^T}(F\dot{\tilde{\mathbf{q}}} + \dot{\tilde{\boldsymbol{\omega}}}) \tag{5.68}$$

and using the *equation (5.22)* for $\dot{\tilde{\boldsymbol{\omega}}}$ the *equation (5.68)* becomes

$$\dot{V} = \mathbf{s^T}\underline{I_s}^{-1}(-\underline{S}(\boldsymbol{\omega})\underline{I_s}\boldsymbol{\omega} - \underline{S}(\boldsymbol{\omega})\mathbf{h_{rw}} - \mathbf{N_{rw}} + \mathbf{N}_{dis} - \underline{I_s}\dot{\bar{\boldsymbol{\omega}}} + \underline{I_s}\underline{F}\dot{\tilde{\mathbf{q}}}) \tag{5.69}$$

where $\bar{\boldsymbol{\omega}}$ is the desired angular velocity. Choosing a control law as:

$$\mathbf{N_{rw}} = -\underline{S}(\boldsymbol{\omega})\underline{I_s}\boldsymbol{\omega} - \underline{S}(\boldsymbol{\omega})\mathbf{h}_{rw} - \underline{I_s}\dot{\boldsymbol{\omega}} + I_s\underline{F}\dot{\tilde{\mathbf{q}}} + \underline{I_s}\lambda sign(\mathbf{s}) \tag{5.70}$$

The *equation (5.69)* is written as:

$$\dot{V} = -\mathbf{s^T}(-\dot{\tilde{\boldsymbol{\omega}}} + \lambda sign(\mathbf{s}) - \mathbf{N}_{dis}) \tag{5.71}$$

Therefore, with $\lambda > ||\dot{\tilde{\boldsymbol{\omega}}}_{max}|| + ||\mathbf{N}_{dis}||$, the condition $\dot{V} < 0$ is satisfied. Thus, λ is chosen to be equal to $||\dot{\tilde{\boldsymbol{\omega}}}|| + c$ where c is designed by trial and error to have the desired behaviour of the sliding manifold $\mathbf{s}$ as represented in the figure 5.7

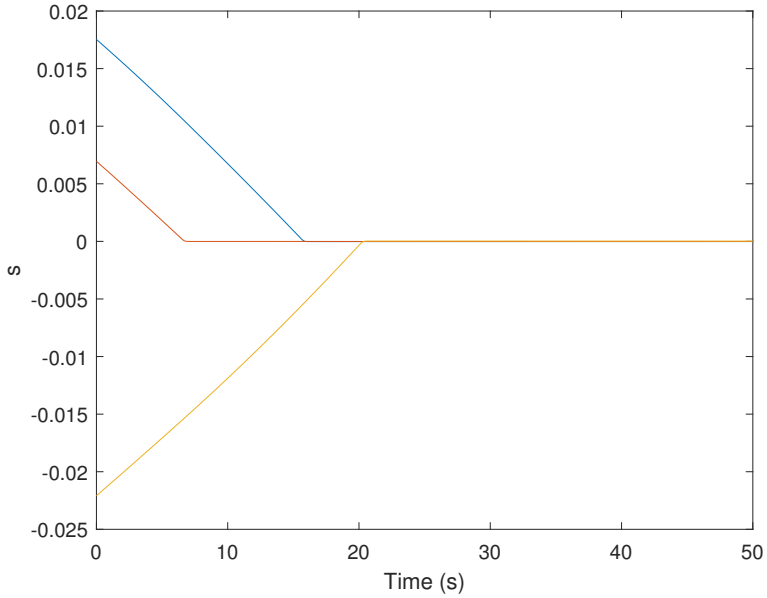

Figure 5.7: $\mathbf{s}$ in function of time with c = 10^{-3}

Sliding mode control suffers from chattering around the manifold. In order to reduce chattering the *sign* function is replaced with the hyperbolic tangent function $tanh(\frac{\mathbf{s}}{\epsilon})$. The same result could be achieved with saturation function $sat(\frac{\mathbf{s}}{\epsilon})$ but with saturation function the simulation of the system is very slow due to singularities. The difference between *sat* and *tanh* is seen in the *figure 5.8*

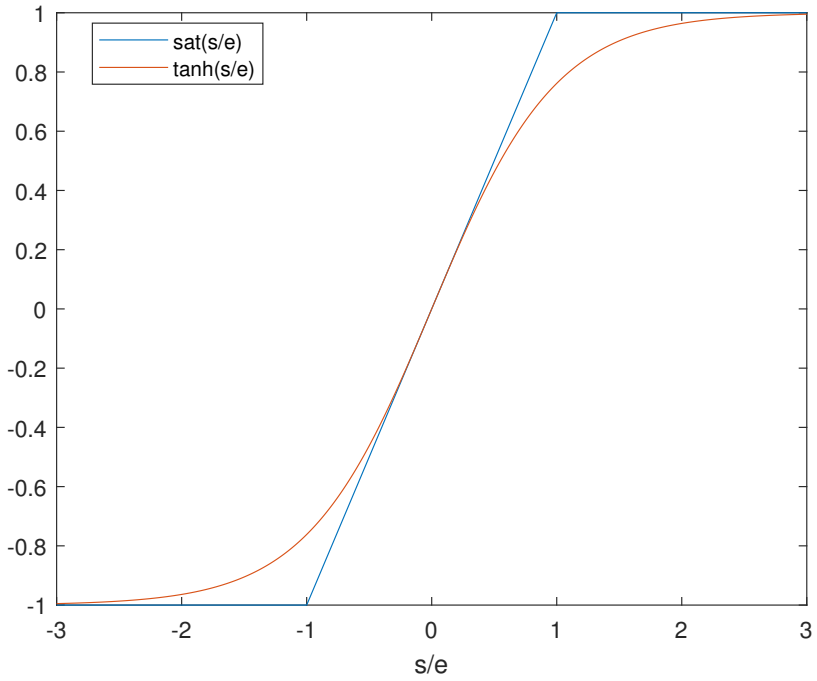

Figure 5.8: Saturation and hyperbolic tangent functions

From the *figure 5.4*, it can be seen that the relative error due to the polynomial fitting is about 10^{-3}. Therefore, a choice of a smaller value for the maximum error quaternion will not influence the total error. Thus, the maximum acceptable error quaternion is chosen to be equal to 10^{-3}. Consequently, the maximum error on $\mathbf{s}$ is equal to $d * 10^{-3} = 3.5 * 10^{-5}$. ϵ is designed by trial and error to set the boundaries of $\mathbf{s}$ inside this maximum acceptable error for the sliding mode variable. The figure 5.9 shows $\mathbf{s}$ in function of time with $\epsilon = 2 * 10^{-3}$.

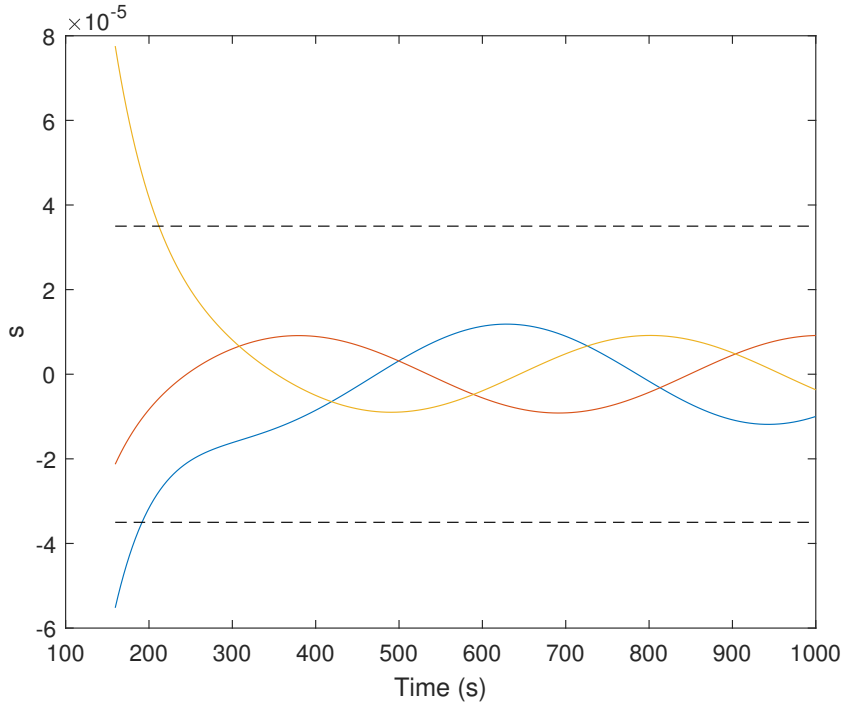

Figure 5.9: **s** in function of time with $\epsilon = 2 * 10^{-3}$

5.4 Simulation and results

The simulation of the state feedback control and sliding mode control are shown in the figure 5.10 and figure 5.11 respectively. At the beginning, the drag force reference is chosen to be equal to the minimum and after 500 seconds alters to the maximum.

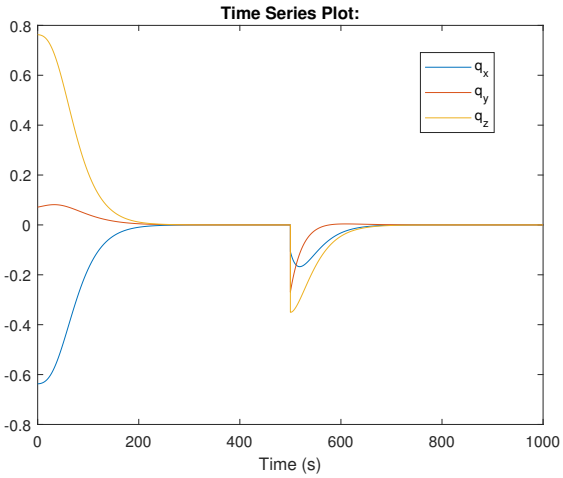

Figure 5.10: Simulation of the state feedback control

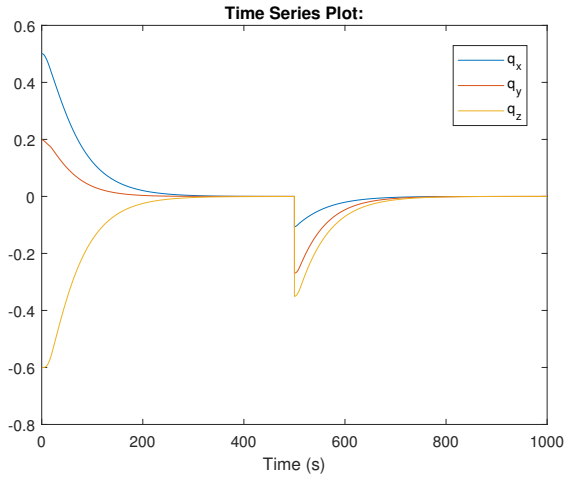

Figure 5.11: Simulation of the sliding mode control

It can be seen that, in the simulation of the state feedback control, the error increases sometimes due to the fact that the linear controller does not take into account the non-linearities of the system. However, in the simulation of sliding mode control, the error quaternion converges as expected.

6 | Acceptance test

The system is tested to see if it fulfils the requirements put up (*chapter 3*).

1. The formation shall be able to maintain a given angle within 45°.

The results from global algorithm illustrated in *figure 4.16* and from distributed algorithm *figure 4.15* show that the requirement is fulfilled. In both figures, it can be seen that the satellites started at the same point and in the end, they are in a flying formation where the angles between them are nearly 45°.

2. Each satellite shall be able to change its orientation.

For this requirement, a linear and nonlinear controller have been designed. The results of these two controllers are shown in *figure 5.10* and in *figure 5.11*, where both are performing well. The satellite is able to track a reference orientation, therefore, the requirement is fulfilled.

7 | Conclusion

The overall objective of this project was to consider several satellites flying in formation with the purpose of pointing towards a target. In order to reach this goal, two controllers were designed: one for controlling the angle between satellites using the drag force and another one for attitude control in order to be able to rotate the satellite to the desired orientation.

First, for designing a controller for the angle, the relative dynamics between two satellites are analyzed. Therefore, an LQR controller is implemented to control the angle between two satellites. The simulations showed that the LQR performed properly. Additionally, two algorithms for formation control are designed, a global and distributed algorithm. Both algorithms are working as intended, where the angles between neighbour satellites converged to the desired angle of 45°, with the mention that in the distributed algorithm case the convergence rate will be slower compared with the global algorithm.

Afterwards, two control methods to obtain the desired orientation of the satellite has been implemented. The first method is a state feedback which is a linear control method. For implementing this controller the equation of motion need to be linearized. The second method is using a non-linear control method called sliding mode control. The results from sliding mode control showed that the error quaternion converged better compared to state feedback control, but in this case, the state feedback is deemed to be more suitable. Besides, the sliding mode convergence is better, but due to the fact that the control law is more complex, the satellite controller will need more computation time.

In conclusion, some acceptance tests have been made to establish that the requirements accomplished.

A | Derivation of relative dynamics equations

The vector position from the centre of the Earth to the satellite 1 and the satellite 2 is given by

$$\mathbf{p_1} = R\hat{\mathbf{x}} \tag{A.1}$$
$$\mathbf{p_2} = R\hat{\mathbf{x}} + x\hat{\mathbf{x}} + y\hat{\mathbf{y}} \tag{A.2}$$

the first time derivative and second time relative of $\mathbf{p_1}$ and $\mathbf{p_2}$ is computed:

$$\dot{\mathbf{p}}_\mathbf{1} = \dot{R}\hat{\mathbf{x}} + R(\mathbf{w} \times \hat{\mathbf{x}})$$

where $\mathbf{w}$ is the angular velocity vector and $\mathbf{w} = w\hat{\mathbf{z}}$ due to the fact the position of the satellites stay all over the time in the plan $(\hat{\mathbf{x}}, \hat{\mathbf{y}})$. Therefore, the first time derivative and the second time derivative are given by:

$$\begin{aligned}
vec\dot{p}_1 &= \dot{R}\hat{\mathbf{x}} + wR\hat{\mathbf{y}} \\
\ddot{\mathbf{p}}_\mathbf{1} &= \ddot{R}\hat{\mathbf{x}} + w\dot{R}\hat{\mathbf{y}} + \dot{w}R\hat{\mathbf{y}} + w\dot{R}\hat{\mathbf{y}} + wR(\mathbf{w} \times \hat{\mathbf{y}}) \\
&= \ddot{R}\hat{\mathbf{x}} + 2w\dot{R}\hat{\mathbf{y}} - w^2R\hat{\mathbf{x}} \\
\dot{\mathbf{p}}_\mathbf{2} &= \dot{\mathbf{p}}_\mathbf{1} + \dot{x}\hat{\mathbf{x}} + xw\hat{\mathbf{y}} + \dot{y}\hat{\mathbf{y}} - yw\hat{\mathbf{x}} \\
&= \dot{\mathbf{p}}_\mathbf{1} + (\dot{x} - yw)\hat{\mathbf{x}} + (xw + \dot{y})\hat{\mathbf{y}} \\
\ddot{\mathbf{p}}_\mathbf{2} &= \ddot{\mathbf{p}}_\mathbf{1} + (\ddot{x} - \dot{y}w - y\dot{w})\hat{\mathbf{x}} + (\dot{x} - yw)w\hat{\mathbf{y}} + (\dot{x}w + x\dot{w} + \ddot{y})\hat{\mathbf{y}} - (xw + \dot{y})w\hat{\mathbf{x}} \\
&= \ddot{\mathbf{p}}_\mathbf{1} + (\ddot{x} - 2\dot{y}w - y\dot{w} - xw^2)\hat{\mathbf{x}} + (\ddot{y} + 2\dot{x}w + x\dot{w} - yw^2)\hat{\mathbf{y}}
\end{aligned}$$

Furthermore, The Newton law gives:

$$m\ddot{\mathbf{p}}_\mathbf{1} = \mathbf{F_{grav,1}} + \mathbf{F_{drag,1}} + \mathbf{F_{dist,1}} \tag{A.3}$$
$$m\ddot{\mathbf{p}}_\mathbf{2} = \mathbf{F_{grav,2}} + \mathbf{F_{drag,2}} + \mathbf{F_{dist,2}} \tag{A.4}$$
$$\Rightarrow \ddot{\mathbf{p}}_\mathbf{2} - \ddot{\mathbf{p}}_\mathbf{2} = \frac{1}{m}(\Delta\mathbf{F_{grav}} + \Delta\mathbf{F_{drag}} + \Delta\mathbf{F}_{dist}) \tag{A.5}$$

with m is the mass of both satellites. The gravity is given by the universal law of gravitation:

$$\frac{\mathbf{F_{grav,1}}}{m} = -G\frac{m_{earth}}{||\mathbf{R}||^3}\mathbf{R}$$
$$\frac{\mathbf{F_{grav,2}}}{m} = -G\frac{m_{earth}}{||\mathbf{R} + \mathbf{r}||^3}(\mathbf{R} + \mathbf{r})$$

where $\mathbf{r} = (x, y)$ is the vector from the satellite 1 to the satellite 2. The denominateur can be approximated using:

$$||\mathbf{R} + \mathbf{r}||^{-3} = ||\mathbf{r}||$$

and thus, the difference between the gravity force on satellite 2 and the the gravity force on 1 is:

$$\mathbf{F_{grav,2}} - \mathbf{F_{grav,1}} \approx -\frac{\mu}{R^3}\mathbf{r}$$

with $\mu = Gm_{earth}$, The drag force can be modelling be using *equation (4.4)*:

$$\begin{aligned}
\mathbf{F_{drag,1}} &= -u_1||\dot{\mathbf{p}}_\mathbf{1}||\dot{\mathbf{p}}_\mathbf{1} \\
&= -u_1||\dot{\mathbf{p}}_\mathbf{1}||(\dot{R}\hat{\mathbf{x}} + wR\hat{\mathbf{y}}) \\
\mathbf{F_{drag,2}} &= -u_2||\dot{\mathbf{p}}_\mathbf{2}||\dot{\mathbf{p}}_\mathbf{2} \\
&= -u_2||\dot{\mathbf{p}}_\mathbf{2}||((\dot{R} + \dot{x} - yw)\hat{\mathbf{x}} + (wR + xw + \dot{y})\hat{\mathbf{y}})
\end{aligned}$$

Therefore, the *equation (A.3)* becomes:

$$\begin{cases}
\ddot{R} - w^2R = -\dfrac{\mu}{R^2} - \dfrac{u_1}{m}||\dot{\mathbf{p}}_\mathbf{1}||\dot{R} + \dfrac{F_{dist,1,x}}{m} \\
2w\dot{R} + \dot{w}R = -\dfrac{u_1}{m}||\dot{\mathbf{p}}_\mathbf{1}||wR + \dfrac{F_{dist,1,y}}{m}
\end{cases} \tag{A.6}$$

and the *equation (A.5)* gives:

$$\begin{cases}
\ddot{x} - 2\dot{y}w - y\dot{w} - xw^2 = -x\dfrac{\mu}{R^3} + \dfrac{u_1}{m}||\dot{\mathbf{p}}_\mathbf{1}||\dot{R} - \dfrac{u_2}{m}||\dot{\mathbf{p}}_\mathbf{2}||(\dot{R} + \dot{x} - yw) + \dfrac{\Delta F_{dist,x}}{m} \\
\ddot{y} + 2\dot{x}w + x\dot{w} - yw^2 = -y\dfrac{\mu}{R^3} + \dfrac{u_1}{m}||\dot{\mathbf{p}}_\mathbf{1}||wR - \dfrac{u_2}{m}||\dot{\mathbf{p}}_\mathbf{2}||(wR + xw + \dot{y}) + \dfrac{\Delta F_{dist,y}}{m}
\end{cases} \tag{A.7}$$

The operating point is the position (x^*, y^*) of the satellite 2 in the frame of satellite. x^* and y^* can be computed from *figure A.1*.

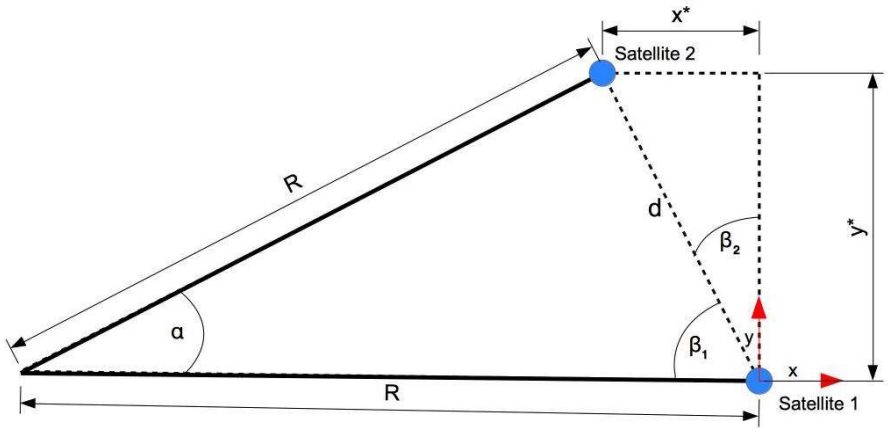

Figure A.1: Operating point

Using trigonometry relations:

$$\begin{aligned} d &= 2Rsin(\frac{\alpha}{2}) \\ x^* &= -dsin(\beta_2) \\ &= -dsin(\frac{\alpha}{2}) \\ &= -2Rsin(\frac{\alpha}{2})^2 \\ y^* &= dcos(\frac{\alpha}{2}) \\ &= 2Rsin(\frac{\alpha}{2})cos(\frac{\alpha}{2}) \\ &= Rsin(\alpha) \end{aligned}$$

with α is the desired angle between satellite and so $\beta_2 = 90° - \beta_1 = 90° - (90° - \frac{\alpha}{2}) = \frac{\alpha}{2}$. Therefore we change the coordinate reference as following:

$$\begin{aligned} x &\Leftarrow x - x^* \\ y &\Leftarrow y - y^* \end{aligned}$$

Thus, the equations *equation (A.7)* become:

$$\begin{cases} \ddot{x} - 2\dot{y}w - (y + y^*)\dot{w} - (x + x^*)w^2 = \\ -(x + x^*)\frac{\mu}{R^3} + \frac{u_1}{m}||\dot{\mathbf{p}}_\mathbf{1}||\dot{R} - \frac{u_2}{m}||\dot{\mathbf{p}}_\mathbf{2}||(\dot{R} + \dot{x} - (y + y^*)w) + \frac{\Delta F_{dist,x}}{m} \\ \ddot{y} + 2\dot{x}w + (x + x^*)\dot{w} - (y + y^*)w^2 = \\ -(y + y^*)\frac{\mu}{R^3} + \frac{u_1}{m}||\dot{\mathbf{p}}_\mathbf{1}||wR - \frac{u_2}{m}||\dot{\mathbf{p}}_\mathbf{2}||(wR + (x + x^*)w + \dot{y}) + \frac{\Delta F_{dist,y}}{m} \end{cases} \tag{A.8}$$

B | Angular velocity equations

The differential equations for R and ω for a satellite is given by the equation (ref B6). In order to find an expression of the angular velocity in function of the drag force, the little perturbation approximation is used for R and ω.

$$R = R_0 - \Delta R \tag{B.1}$$
$$\omega = \omega_0 - \Delta\omega \tag{B.2}$$

where R_0 and ω_0 are the initial value and $\omega_0 = \sqrt{\frac{\mu}{R_0^3}}$. Therefore, the system of equations B6 become:

$$\ddot{\Delta R} - (\omega_0 + \Delta\omega)^2(R_0 + \Delta R) = -\frac{\mu}{(R_0 + \Delta R)^2} - u\frac{v}{m}\dot{\Delta R} \tag{B.3}$$
$$2(\omega_0 + \Delta\omega)\dot{\Delta R} + \dot{\Delta\omega}(R_0 + \Delta R) = -u\frac{v}{m}(\omega_0 + \Delta\omega)(R_0 + \Delta R) \tag{B.4}$$

The *equation (B.3)* can be simplified using approximations that the speed of the satellites can be assumed constant ($||\dot{\mathbf{p}} = v_0 = \omega_0 R_0$), the second derivative of ΔR is neglectable and by deleting all the second order term. Thus the equation gives:

$$-\omega_0^2 R_0 - 2\omega_0 R_0 \Delta\omega - w_0^2 \Delta R = -\frac{\mu}{R_0^2}(1 + \frac{\Delta R}{R_0})^{-2} - u\frac{v_0}{m}\dot{\Delta R} \tag{B.5}$$
$$\Rightarrow -\omega_0^2 R_0 - 2\omega_0 R_0 \Delta\omega - \omega_0^2 \Delta R = -\omega_0^2 R_0 + 2\omega_0^2 \Delta R - u\frac{v_0}{m}\dot{\Delta R} \tag{B.6}$$
$$\Rightarrow \Delta R = -\frac{2R_0}{3\omega_0}\Delta\omega + u\frac{R_0}{3\omega_0 m}\dot{\Delta R} \tag{B.7}$$
$$\Rightarrow \Delta R \approx -\frac{2R_0}{3\omega_0}\Delta\omega \tag{B.8}$$

because $\frac{u}{m} << 1$. The second equation D.4 can be simplified by neglected the second order term:

$$2\omega_0\dot{\Delta R} + \dot{\Delta\omega}R_0 = -\frac{u}{m}\omega_0^2 R_0^2 \tag{B.9}$$
$$\Rightarrow -\frac{4}{3}R_0\dot{\Delta\omega} + \dot{\Delta\omega}R_0 == -\frac{u}{m}\omega_0^2 R_0^2 \tag{B.10}$$
$$\Rightarrow \dot{\Delta\omega} = \frac{3\omega_0^2 R_0}{m}u \tag{B.11}$$

Thanks to this equation, the angular velocity can be computed in function of the drag force on the satellite.

Bibliography

[1] Marcel J. Sidi. *Spacecraft dynamics and control*. 1st ed. Press Syndicate of the University of Cambridge, 1997.

[2] Kyle Alfriend, Srinivas Vadali, and Pini Gurfil. *Spacecraft formation flying*. 1st ed. Butterworth-Heinemann, 2009.

[3] Danwei Wang, Baolin Wu, and Eng Kee Poh. *Satellite formation flying*. 1st ed. Springer, 2017.

[4] AAU. *AAU Space*. Oct. 23, 2010. URL: http://www.space.aau.dk/aausat3 (visited on 10/26/2017).

[5] California Polytechnic State University. *CubeSat Design Specification*. 1st ed. Springer, 2014.

[6] California Polytechnic State University. *Poly Picosatellite Orbital Deployer Mk. III Rev. E*. 1st ed. Springer, 2014.

[7] eoPortal Directory. *ESTCube-1*. Oct. 23, 2010. URL: https://directory.eoportal.org/web/eoportal/satellite-missions/e/estcube-1 (visited on 10/26/2017).

[8] F. Landis Markley and John L. Crassidis. *Fundamentals of Spacecraft Attitude Determination and Control*. 1st ed. Springer, 2014.

[9] Wikipedia. *Drag coefficient*. Oct. 23, 2010. URL: https://en.wikipedia.org/wiki/Drag_coefficient (visited on 12/15/2015).

[10] James R. Wertz. *Spacecraft attitude determination and control*. 7th ed. KluwerAcademicPublisher, 1984.

[11] Eze Charles U., Dr Mbaocha Christian C, and Dr Onojo James O. *Design of Linear Quadratic Regulator for the Three-Axis Attitude Control System Stabilization of Microsatellites*. 2016. URL: https://www.ijser.org/researchpaper/Design-of-Linear-Quadratic-Regulator-for-the-Three-Axis-Attitude-Control-System-Stabilization-of-Microsatellites.pdf (visited on 12/15/2017).

[12] Kasper Fuglsang Jensen and Kasper Vinther. *Attitude Determination and Control System for AAUSAT3*. Aalborg University, 2010.

[13] Michel Capderou. *Satellites Orbits and Missions*. 1st ed. Springer, 2005.

[14] Corentin Briat. *Linear Parameter Varying and Time-Delay Systems*. 1st ed. Springer, 2015.

[15] Wisniewski Rafal. *Satellite Attitude Control Using Only Electromagnetic Actuation*. 1st ed. Aalborg University, 1997.

[16] Peijun Yu, Keqiang Xia, and Jiancheng Li. *A Design of Reconfigurable Satellite Control System with Reaction Wheels Based on Error Quaternion Model*. 2011. URL: https://www.ijser.org/researchpaper/Design-of-Linear-Quadratic-Regulator-for-the-Three-Axis-Attitude-Control-System-Stabilization-of-Microsatellites.pdf (visited on 12/15/2017).